# Computational Physics Course Project
# Equilibration and "Thermalization" in the Adapted Caldeira–Leggett Model

Zixi Xia (PB22000057)
Email: xzx1602@mail.ustc.edu.cn
School of the Gifted Young, University of Science and Technology of China

*Date: February 17, 2025*

**Abstract**

This report is the reproduction of paper [1] and investigates the equilibration process within the Adapted Caldeira-Leggett (ACL) model. The ACL model is a simple model ("toy model") capable of numerical computation, designed to study quantum decoherence phenomena between a harmonic oscillator and its environment. Under certain parameters, the system reflects properties of "thermalization". This property is related to the intrinsic nature of the global eigenstates and also serves as a microcosm of ergodic behavior found in much larger real systems.

**Keywords:** Equilibration; Thermalization; Quantum Entanglement; Closed Systems; Finite Systems

Note: This report is an English translation of the original Chinese manuscript; please be aware that potential translation errors or terminological discrepancies may exist.

## 1 Introduction

Andreas Albrecht and Rose Baunach proposed the ACL model in a paper published on arXiv in 2021 ([2], published in the formal journal *Physical Review Research* in 2023, later than the publication of paper [1]). This model is used to observe decoherence and environment-induced superselection (einselection [13]) between a harmonic oscillator and its environment, and it is easier to solve numerically compared to the Caldeira-Leggett model [7]. The ACL model naturally evolves towards an equilibrium state over time. In another paper [3] by the author Andreas Albrecht, he obtained an equilibrium state; to investigate whether the ACL model can support this equilibrium state, he wrote the paper [1], which is the subject of this study.

This report investigates the equilibrium states in the ACL model in greater depth. Various equilibration behaviors are feasible, some of which exhibit behavior similar to "thermalization". The setting of initial parameters determines whether the system will display "thermalization" or other behaviors. In

its design, the ACL model embodies a series of actual physical properties and can effectively calculate decoherence phenomena with limited computational cost.

Often, certain properties of extremely large quantum systems are determined by only a few quantities (e.g., in the CL model, although each oscillator can have distinct angular frequencies, masses, etc., the overall behavior is determined solely by quantities such as $B(t)$ and $\gamma(t)$, see Section 5.1, as well as [4, 5]). This is because processes such as "equilibration" and "thermalization" wipe out some degrees of freedom during evolution. What kind of systems exhibit this phenomenon? This report explores some behaviors within the ACL model.

# 2 Main Models and Computational Methods

## 2.1 Adapted Caldeira-Leggett Model

The standard Caldeira-Leggett model can be expressed as ([7], see Section 5.1 for relevant conclusions):

$$H = H_A + H_I + H_B = \frac{p^2}{2M} + v(x) + x\sum_k C_k R_k + \sum_k \frac{p_k^2}{2m} + \sum_k \frac{1}{2} m\omega_k^2 R_k^2 \tag{1}$$

Its physical significance is: a particle in a potential field (the central particle) is subjected to linear coupling interactions from a series of environmental (referred to as the *Reservoir* in the paper) harmonic oscillators. $C_k$ is the coupling constant, and $\omega_k$ is the oscillation frequency of the environmental particles.

The biggest challenge with the CL model is the difficulty in numerical solution. The Adapted Caldeira-Leggett model (ACL model [2]) uses approximation methods to transform the solution space into a finite-dimensional Hilbert space. Considering the Hilbert space of the central particle (referred to as the *system* in the paper) as $s$ and the Hilbert space of the external environment as $e$, the total Hilbert space is represented as the tensor product $s \otimes e$ (see Section 5.3 for details on the tensor product). Analogous to the CL model Eq. 1, the global (referred to as the *world* in the paper) Hamiltonian $H_w$ can also be divided into three parts:

$$H_w = H_s \otimes \mathbf{1}^e + H^I + \mathbf{1}^s \otimes H_e \tag{2}$$

where $H^I = q_s \otimes H_e^I$ is the interaction term between the central particle and the environment, and $q_s$ is the coordinate of the central particle (like the CL model, this model is also one-dimensional).

Paper [2] provides a diagram describing the interaction between the environmental state and the harmonic oscillator state, as shown in Figure 1.

The wavefunction of the central particle is decomposed using the energy eigenstates of the simple harmonic oscillator to form the Hilbert space $s$; its properties are detailed in Section 5.2. The interaction term and the environment self-term are respectively:

$$H_e^I = E_I R_L^e + E_I^0, \qquad H_e = E_e R^e + E_e^0 \tag{3}$$

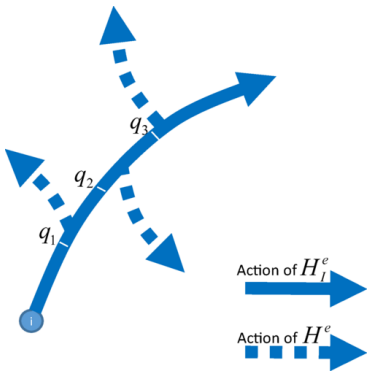


**Figure 1:** The interaction term $q_s \otimes H_e^I$ can move the environmental state along a path determined by $H_e^I$ (labeled incorrectly in the figure), indicated by the solid line. If the number of $q$ states capable of coupling with the environmental state increases, the rate of this transition also increases. If $[H_e^I, H_e] \neq 0$, then $H_e$ can act to deviate the evolution from the aforementioned path, with the degree of deviation related to the starting point (proportional to $q$), indicated by the dashed line. Some invariant properties can effectively accelerate computational efficiency. Adapted from Figure 1 in Reference [2].

### 2.1.1 Quantifying the Degree of Entanglement between System and Environment: von Neumann Entropy

The initial state of the system can be represented as the product of the environment state and the system state, which is a pure state. Define the density matrices:

$$\rho_s = Tr_e(|\psi\rangle\langle\psi|), \rho_e = Tr_s(|\psi\rangle\langle\psi|), \rho_w = |\psi\rangle\langle\psi|$$

This is the result of taking the partial trace (environment/system) of the total density matrix. Define the von Neumann entropy (the formula in [2] is incorrect):

$$S = -tr(\rho_s \ln \rho_s) = -tr(\rho_e \ln \rho_e) \tag{4}$$

Since for any state $|\phi\rangle$,

$$\langle\phi|\rho_{s/e}|\phi\rangle = \langle\phi|_{s/e}|\psi\rangle_{s/e}\langle\psi|_{s/e}|\phi\rangle_{s/e}$$

is a non-negative real number (the subscript indicates the component of the state in the subspace), implying that the density matrix is positive (semi-)definite. Thus, the entropy is numerically equal to ($\lambda_i$ are the eigenvalues of $\rho_s$ or $\rho_e$; note that $0 \ln 0 = 0$)

$$S = -\sum_i \lambda_i \ln \lambda_i$$

Let the dimensions of $\rho_s$ and $\rho_e$ be $N_s$ and $N_e$ respectively (corresponding to the dimensions of the Hilbert subspaces), then the maximum value of entropy is:

$$S_{max} = \ln(\min(N_s, N_e));$$

If we denote $N = \min(N_s, N_e)$, then for the entropy to take the maximum value, all eigenvalues should be $\frac{1}{N}$, and the density matrix is

$$\rho = \frac{1}{N} I_n$$

The subscript is the same as the subspace corresponding to $N$.

### 2.1.2 Energy Distribution

Define the energy probability:

$$P_s(E) = diag(\rho_s^E), P_e(E) = diag(\rho_e^E)$$

This indicates the probability of being at energy $E$ ($E$ generally can only take the harmonic oscillator eigenenergy or the environment eigenstate energy). Here, the "diagonal terms" should use eigenstates as the basis, requiring a basis transformation of the state during the solution process.

Similarly, using global eigenstates as the basis, the global energy probability can also be defined:

$$P_w(E) = diag(\rho_w^E) = diag(|\psi\rangle_w \langle\psi|_w)$$

### 2.1.3 Effective Dimension

Paper [1] defines the effective dimension as ($E_i$ is the global energy eigenvalue):

$$d_{eff}^w = \frac{1}{\sum_i (P_w(E_i))^2} \tag{5}$$

Since $\sum_i P_w(E_i) = 1$, in the above equation

$$\sum_i (P_w(E_i))^2 \geq \frac{(\sum_i P_w(E_i)^2}{N_w} = \frac{1}{N_w}$$

where $N_w = N_s N_e$ refers to the dimension of the total Hilbert space. This shows that the maximum effective dimension is $N_w$, and the condition for equality is that the quantum state has equal probability on every energy eigenstate.

## 2.2 Computational Methods

### 2.2.1 Nondimensionalization

Let $\hbar = 1, m = 1, \omega = 1$. Then the harmonic oscillator energy eigenvalues are $E_n = n + \frac{1}{2}$, and the coordinate can be expressed as $q_s = \frac{1}{\sqrt{2}}(a + a^\dagger)$. The coordinate matrix element of the coherent state (see Section 5.2.1) can also be expressed as (Eq. 15):

$$\langle\alpha(t)| q_s |\alpha(t)\rangle = \frac{1}{\sqrt{2}}(\alpha e^{-i\omega t} + \overline{\alpha} e^{i\omega t}) = \sqrt{2}|\alpha| \cos(\omega t - \arg(\alpha))$$

### 2.2.2 Hilbert Space and Hamiltonian

In actual calculations, the infinite-dimensional Hilbert space of harmonic oscillator eigenstates cannot be handled, requiring truncation. Assuming the truncation results in only $N_s$ eigenstates, the difference from the untruncated harmonic oscillator lies in:

$$a^\dagger |N_s - 1\rangle = 0 |\rangle$$

$a^\dagger$ is the raising (creation) operator. In the paper, it is manifested as (slightly different from the form in the paper):

$$[a, a^\dagger] = 1 + \Delta, \qquad \langle i| \Delta |j\rangle = -N_s \delta_{i,N_s-1} \delta_{j,N_s-1}$$

The proof is as follows:

$$\begin{aligned}\langle N_s-1|\,\Delta\,|N_s-1\rangle =& \langle N_s-1|\,(aa^\dagger - a^\dagger a - 1)\,|N_s-1\rangle \\ =& \langle N_s-1|\,0\,|\rangle - (\sqrt{N_s-1}\,|N_s-2\rangle)^\dagger(\sqrt{N_s-1}\,|N_s-2\rangle) - 1 \\ =& 1 - N_s - 1 = -N_s\end{aligned}$$

In actual calculations, $N_s = 30$ is taken, meaning only states with quantum numbers $0 \sim 29$ are retained.

Since the quantum state of the "environment" is uncertain, assume it can be expanded under a set of basis vectors (corresponding to Hilbert space $e$), taking dimension $N_e = 600$. Then the total Hilbert space is obtained by the tensor product of the two, with dimension $N_w = 18000$.

Considering random interactions, let $R_I^e$ and $R^e$ be random Hermitian matrices (real and imaginary parts of independent elements are uniformly distributed on $[-0.5, 0.5]$), which do not change with time; $E_l$ and $E_e$ are scalars scaling the energy. For convenience, assume bias terms $E_I^0 = 0$ and $E_e^0 = 0$.

### 2.2.3 Selection of Initial States (see also Appendix A of paper [1])

The coherent state $|\alpha\rangle_s = \exp(\alpha a^\dagger - \overline{\alpha}a)\,|0\rangle_s$ can maintain wave-like motion well without wave-function spreading (see Section 5.2.1), while corresponding to the simple harmonic motion of a harmonic oscillator in the classical case. In the CL model, the central particle is a classical harmonic oscillator; for comparison, the ACL model uses a coherent state as the initial state of the central particle.

For the environmental state, the eigenstates of $H_e$ are selected. To achieve a distribution as random as possible, the paper selects the $i \in 300, 400, 450, 500, 550$-th eigenstates $|i\rangle_e$ (sorted by eigenvalue from small to large) as five initial states. In practice, due to randomness, the eigenenergy distribution is almost uniform; the 300th eigenenergy is close to 0, and the rest increase.

The paper also adjusts the selection of the coherent state $|\alpha\rangle_s$ based on the environmental state so that the total energy $(\langle i|_e \langle\alpha|_s) H_w (|\alpha\rangle_s |i\rangle_e) = 25$. Expanding gives:

$$25 = (\langle i|_e \langle\alpha|_s) H_w (|\alpha\rangle_s |i\rangle_e) = \langle\alpha|_s H_s |\alpha\rangle_s + \langle\alpha|_s q_s |\alpha\rangle_s \langle i|_e H_e^I |i\rangle_e + \langle i|_e H_e |i\rangle_e$$

Since $|i\rangle_e$ is already solved, its matrix elements can be directly determined. The matrix elements regarding the coherent state are as follows:

$$\begin{aligned}\langle\alpha|_s H_s |\alpha\rangle_s =& \sum_{n=0}^{\infty} e^{-\overline{\alpha}\alpha}\frac{(\overline{\alpha}\alpha)^n}{n!}\left(n+\frac{1}{2}\right) \\ =& \frac{1}{2}\sum_{n=0}^{\infty} e^{-\overline{\alpha}\alpha}\frac{(\overline{\alpha}\alpha)^n}{n!} + \overline{\alpha}\alpha\sum_{n=1}^{\infty} e^{-\overline{\alpha}\alpha}\frac{(\overline{\alpha}\alpha)^{n-1}}{(n-1)!} \\ =& \overline{\alpha}\alpha + \frac{1}{2} \qquad \text{Normalization: } \sum_{n=0}^{\infty} e^{-\overline{\alpha}\alpha}\frac{(\overline{\alpha}\alpha)^n}{n!} = 1\end{aligned}$$

And (initial state $t = 0$):

$$\langle\alpha|_s q_s |\alpha\rangle_s = \frac{1}{\sqrt{2}}(\alpha + \overline{\alpha}) = \sqrt{2}\Re(\alpha)$$

Assuming $\alpha$ is a real number, we get the equation:

$$\alpha^2 + (\sqrt{2}\,\langle i|_e H_e^I |i\rangle_e)\alpha + (\langle i|_e H_e |i\rangle_e - \frac{49}{2}) = 0 \tag{6}$$

However, in practice, because $\langle H_w \rangle = 25$ is required, in some cases (e.g., the environmental eigenstate with $i = 300$, plus a minimal interaction term), the initial energy representing the harmonic oscillator should be around 25. This means states near quantum number $n = 25$ occupy a high proportion. Truncating to $N_s = 0 \sim 29$ while using the above approximation method is unreasonable. Therefore, the calculation method should be modified, and infinite summation cannot be used for approximation.

To ensure normalization, the coherent state is: $|\alpha\rangle = \frac{\sum_{n=0}^{29} \frac{\alpha^n}{\sqrt{n!}} |n\rangle}{\sqrt{\sum_{n=0}^{29} \frac{(\overline{\alpha}\alpha)^n}{n!}}}$. Substituting yields ($\hbar\omega = 1$):

$$\langle\alpha|_s H_s |\alpha\rangle_s = \frac{\sum_{n=0}^{29} \frac{(\overline{\alpha}\alpha)^n}{n!}\left(n+\frac{1}{2}\right)}{\sum_{n=0}^{29} \frac{(\overline{\alpha}\alpha)^n}{n!}} = \frac{1}{2} + \overline{\alpha}\alpha \frac{\sum_{n=1}^{29} \frac{(\overline{\alpha}\alpha)^{n-1}}{(n-1)!}}{\sum_{n=0}^{29} \frac{(\overline{\alpha}\alpha)^n}{n!}} = \overline{\alpha}\alpha \left(1 - \frac{1}{29! \sum_{n=0}^{29} \frac{(\overline{\alpha}\alpha)^{n-29}}{n!}}\right) + \frac{1}{2}$$

$$a|\alpha\rangle = \frac{\sum_{n=0}^{29} \frac{\alpha^n}{\sqrt{n!}} a|n\rangle}{\sqrt{\sum_{n=0}^{29} \frac{(\overline{\alpha}\alpha)^n}{n!}}} = \frac{\alpha \sum_{n=1}^{29} \frac{\alpha^{n-1}}{\sqrt{(n-1)!}} |n-1\rangle}{\sqrt{\sum_{n=0}^{29} \frac{(\overline{\alpha}\alpha)^n}{n!}}} = \alpha|\alpha\rangle - \frac{\frac{\alpha^{30}}{\sqrt{29!}}}{\sqrt{\sum_{n=0}^{29} \frac{(\overline{\alpha}\alpha)^n}{n!}}} |29\rangle$$

$$\begin{aligned}
\langle\alpha|_s q_s |\alpha\rangle_s &= \langle\alpha| \frac{1}{\sqrt{2}}(a + a^\dagger) |\alpha\rangle = \sqrt{2}\Re(\langle\alpha| a |\alpha\rangle) \\
&= \sqrt{2}\Re\left(\alpha - \frac{\frac{\alpha^{30}}{\sqrt{29!}} \langle\alpha|29\rangle}{\sqrt{\sum_{n=0}^{29} \frac{(\overline{\alpha}\alpha)^n}{n!}}}\right) = \sqrt{2}\Re\left(\alpha - \frac{\frac{\alpha^{30}}{\sqrt{29!}}}{\sqrt{\sum_{n=0}^{29} \frac{(\overline{\alpha}\alpha)^n}{n!}}} \frac{\frac{\overline{\alpha}^{29}}{\sqrt{29!}}}{\sqrt{\sum_{n=0}^{29} \frac{(\overline{\alpha}\alpha)^n}{n!}}}\right) \\
&= \sqrt{2}\Re\left(\alpha\left(1 - \frac{1}{29! \sum_{n=0}^{29} \frac{(\overline{\alpha}\alpha)^{n-29}}{n!}}\right)\right)
\end{aligned}$$

Let

$$f(\overline{\alpha}\alpha) = 1 - \frac{1}{29! \sum_{n=0}^{29} \frac{(\overline{\alpha}\alpha)^{n-29}}{n!}}$$

Figure 2 shows the graph of $f(\overline{\alpha}\alpha)$, indicating that when $\overline{\alpha}\alpha > 15$, the aforementioned approximation begins to fail, and this factor should be considered.

At this point, solving the quadratic equation becomes solving a univariate nonlinear equation:

$$\left(\alpha^2 + \left(\sqrt{2}\langle i|_e H_e^I |i\rangle_e\right)\alpha\right) f(\alpha) + \langle i|_e H_e |i\rangle_e - \frac{49}{2} = 0 \tag{7}$$

Assuming $\alpha$ is a real number, the root $\alpha$ with the smallest modulus can be found. In actual solving, real solutions always exist.

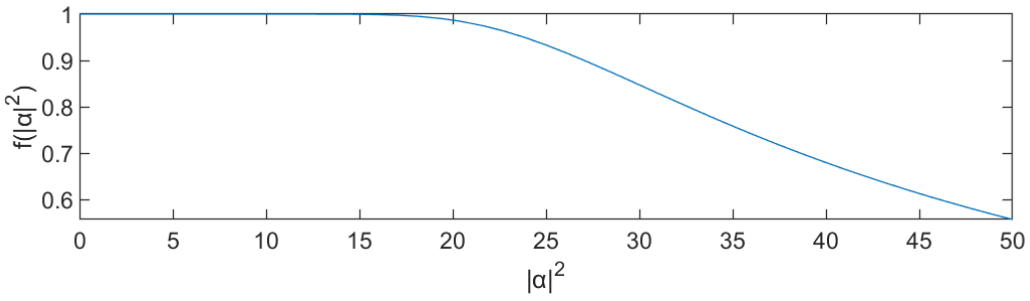


**Figure 2:** Graph of the function $f(\overline{\alpha}\alpha) = 1 - \dfrac{1}{29!\sum_{n=0}^{29}\dfrac{(\overline{\alpha}\alpha)^{n-29}}{n!}}$. When $\overline{\alpha}\alpha > 15$, the approximation starts to fail; at $\overline{\alpha}\alpha = 25$, the error introduced is about 10%.

### 2.2.4 Time Evolution

From the above, the initial state is obtained:

$$|\psi(t=0)]\rangle = |\alpha(t=0)\rangle_s \otimes |i\rangle_e$$

To obtain evolution information, the eigenstates and eigenvectors of $H_w$ also need to be solved (due to the existence of the interaction term $H_I$, the eigenstates are not tensor products of the system and environment; fortunately, $H_w$ is time-independent, so energies and eigenstates are constant). Decompose $|\psi(t=0)\rangle$ onto these eigenstates:

$$|\psi(t=0)\rangle = \sum_i \beta_i |E_i\rangle$$

Then at a certain moment,

$$|\psi(t)\rangle = \sum_i e^{-i\frac{E_i t}{\hbar}} \beta_i |E_i\rangle$$

During the evolution process, the proportions of harmonic oscillator, environment, and interaction energies $\langle H_s\rangle, \langle H_e\rangle, \langle H_I\rangle$ will change.

In practice, the solved eigenvectors are 18000 column vectors, orthogonal and normalized to each other. The matrix form is $\psi(t=0)_{n\times 1} = E_{n\times n}\beta_{n\times 1}$. The matrix $E$ is a unitary matrix, so $\beta = E^\dagger \psi(t=0)$ (matrix form), avoiding matrix inversion.

# 3 Simulation Results

## 3.1 Time Evolution: Equilibration and Decoherence

Let $E_e = 0, E_I = 0.02$ (unless otherwise specified, the same applies below). Select an initial state (using the method in Section 2.2.3, taking the last generated state), simulate the time evolution, and present the energy distribution and entropy at different times, as shown in Figure 3(a,b). It can be seen that energy exchange occurs between the harmonic oscillator and the environment, entropy increases, and then it reaches a stable state with small fluctuations ("Equilibration").

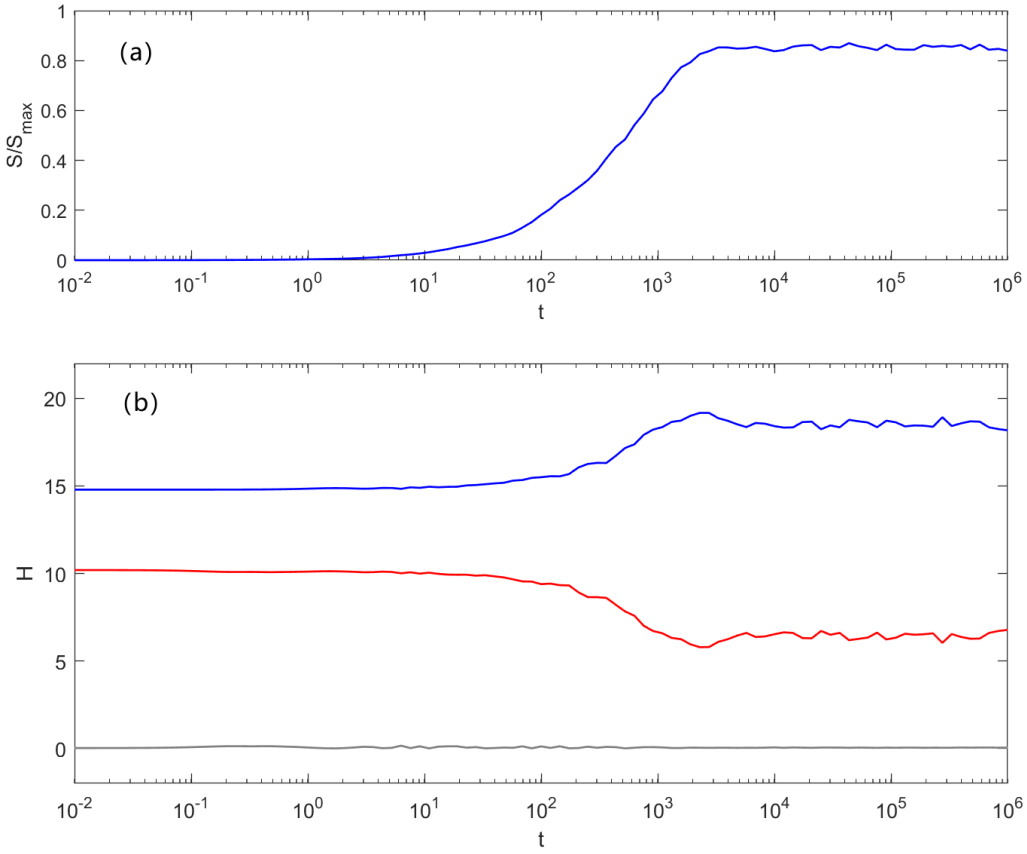


**Figure 3:** Equilibration process in the ACL model: entropy increases, energy flows, and then small fluctuations occur around the steady state. (a) The ratio of the entanglement entropy between the harmonic oscillator and the environment $\frac{S}{S_{max}}$, where $S_{max} = \ln(\min(N_s, N_e)) = \ln 30$; (b) Subsystem energies: $\langle H_s \rangle$ (blue), $\langle H_e \rangle$ (red), and interaction energy $\langle H_I \rangle$ (gray).

What kind of state is the steady state? Due to the action of the factor $e^{-i\frac{E_i t}{\hbar}}$, the phases between different eigenstates become disordered. This indicates a process of "dephasing" (the author of paper [1] points out that "dephasing" refers to the phenomenon where the phase of the eigenstate expansion term $\beta_i(t)$ becomes randomized as time progresses). To verify this idea, we can manually scramble the phases of the state generated in Section 2.2.3 for simulation and compare it with the ordered case to obtain the results in Figure 4. Comparison with Figure 3 verifies that the system produces the so-called dephasing effect as time evolves. This effect is strongly associated with the concept of "decoherence" in quantum statistical mechanics.

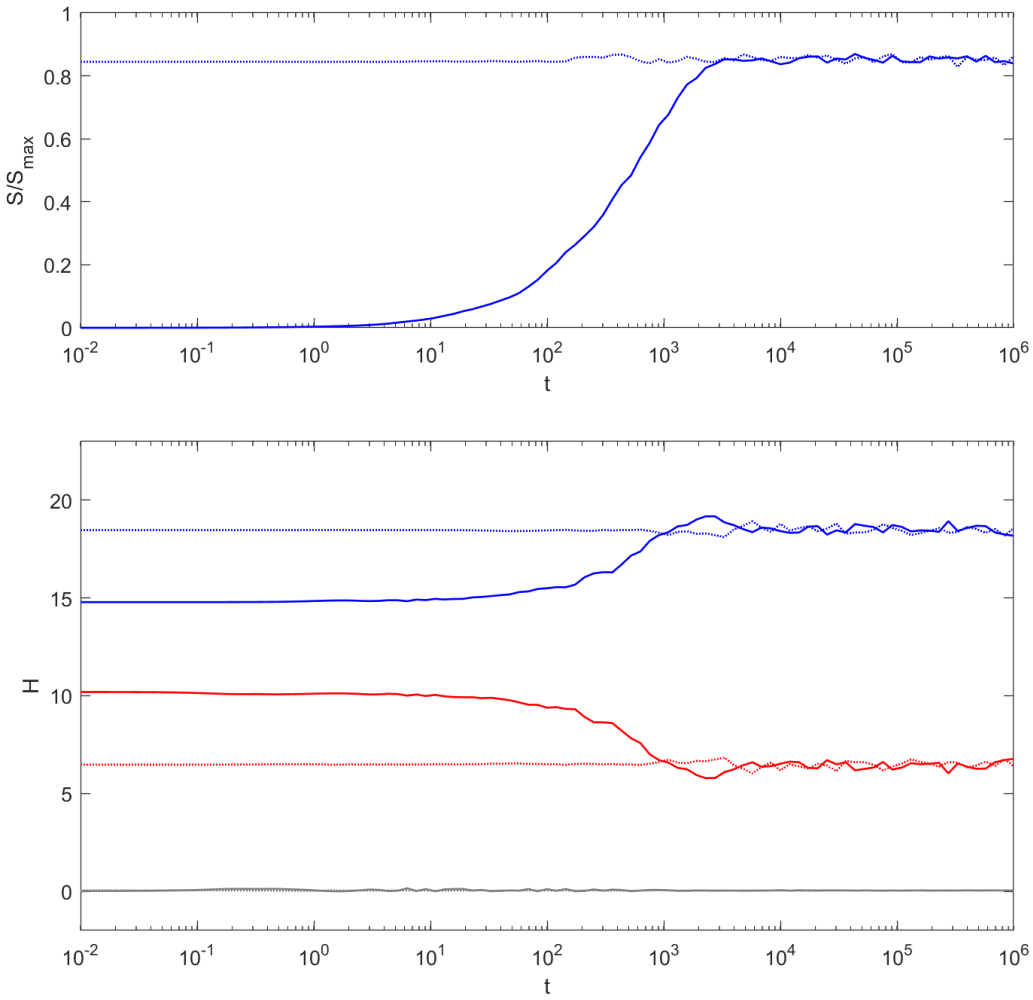


**Figure 4:** Dephasing process: Compared to Figure 3, the case with randomized initial phases (dashed line data) is added. The two coincide after a certain time, indicating that the aforementioned equilibration process possesses dephasing characteristics. Data: $\langle H_s \rangle$ (blue), $\langle H_e \rangle$ (red), $\langle H_I \rangle$ (gray), entropy $\frac{S}{S_{max}}$ (blue).

### 3.2 Equilibrium States without "Thermalization"

Select different initial states (the 5 generated in Section 2.2.3) and present the evolution of energy and entropy over time similar to Figure 3, see Figure 5. The total energy is 25 for all. Although the initial system/environment energies are different, in thermodynamics, two objects with the same total energy will eventually reach the so-called same thermal equilibrium state regardless of their initial temperatures. However, in this case with different initial states, they do not evolve to the same equilibrium state, maintaining a smaller energy difference than originally. The paper also uses the term "thermalize" to describe this.

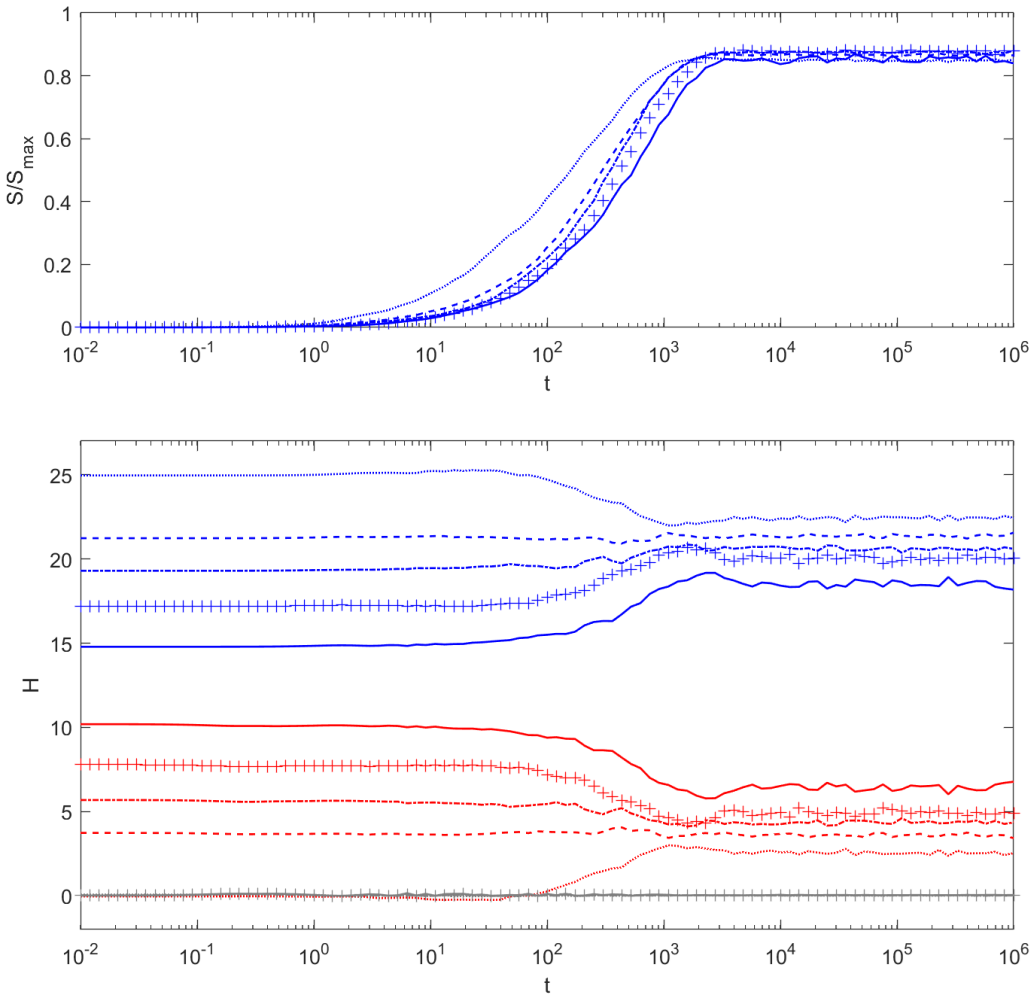


**Figure 5:** Results under different initial conditions (represented by different line styles, where the solid line corresponds to the state in Figure 3). These initial conditions maintain the same total energy as the results in Figure 3. Unlike thermodynamic equilibrium, different initial conditions yield different equilibrium states. Data: $\langle H_s \rangle$ (blue), $\langle H_e \rangle$ (red), $\langle H_I \rangle$ (gray), entropy $\frac{S}{S_{max}}$ (blue).

### 3.3 Impact of Randomness

Maintain $E_e = 0, E_I = 0.02$, use different random numbers to generate $H_e$ and $H_e^I$, perform the same operations as in Section 3.1 (same selection method for the initial state), and also perform the test of manually scrambling phases. Plotting them on one graph, see Figure 6, it is evident that randomness has almost no effect on the initial and final states, only slightly affecting the intermediate evolution process, reflecting the same physical phenomenon.

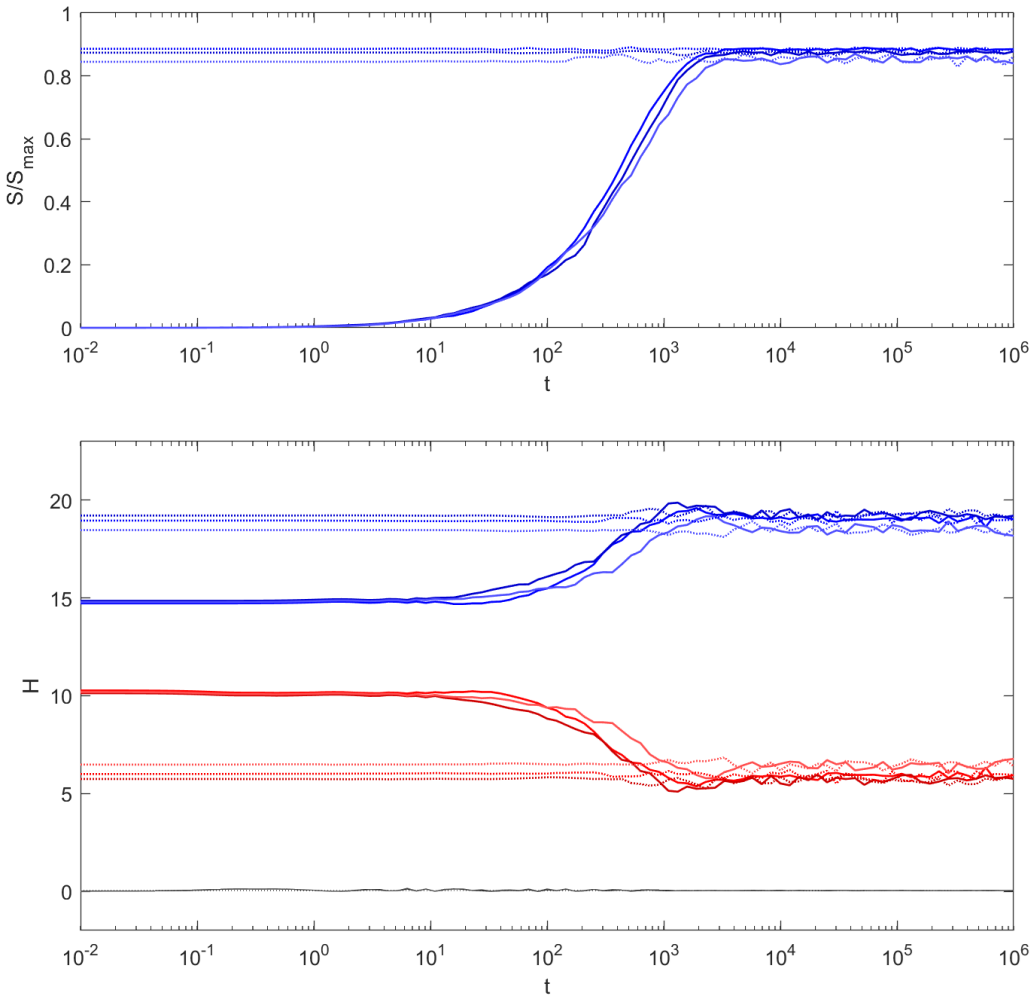


**Figure 6:** Impact of Randomness: Different curves in the figure correspond to evolution results using several sets of $H_e, H_e^I$ generated by different random numbers, as well as their evolution results after scrambling the phases of the initial states. These results converge to nearly consistent values, indicating that the changes in the Hamiltonian brought about by randomness only lead to minor deviations in the results. Data: $\langle H_s \rangle$ (blue), $\langle H_e \rangle$ (red), $\langle H_I \rangle$ (gray), entropy $\frac{S}{S_{max}}$ (blue).

### 3.4 Different Coupling Strengths $E_I$

If we consider the case where $E_I = 0$, there is no energy flow between the environment and the harmonic oscillator, and their respective energies $\langle H_e \rangle, \langle H_s \rangle$ are conserved. The initial state (coherent state + environmental eigenstate) has already reached "equilibrium". Due to the properties of coherent states (see Section 5.2.1), this initial state will not change even after evolving for a sufficiently long time. This can to some extent explain the reason for not achieving "thermalization" in Figure 5.

First, select $E_I = 0.007$, with other selections being the same as before. The results obtained are shown in Figure 7. The energy changes of the two subsystems are very small, making the energy at equilibrium highly dependent on the initial energy, similar to the $E_I = 0$ case. The author of paper [1] believes this does not imply that equilibrium takes longer for smaller $E_I$; if "thermalization" is required, a larger system state might be needed to support the calculation.

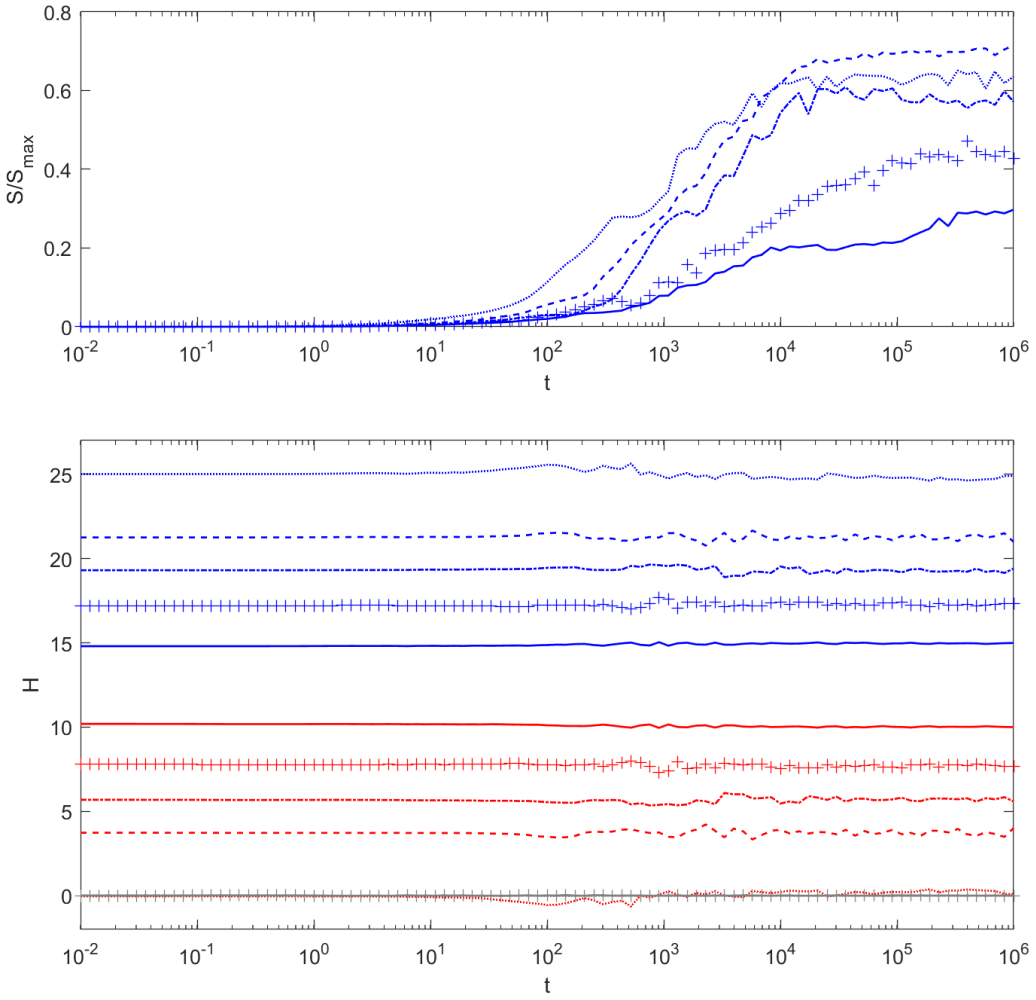


**Figure 7:** Figure 5 when $E_I = 0.007$. The energy flow is much smaller, and the energy difference between subsystems in different equilibrium states increases, approximating the $E_I = 0$ limit. Data: $\langle H_s \rangle$ (blue), $\langle H_e \rangle$ (red), $\langle H_I \rangle$ (gray), entropy $\frac{S}{S_{max}}$ (blue).

Figure 8 shows the case for $E_I = 0.1$. The stronger coupling between the environment and the system leads to signs of "thermalization". Meanwhile, the interaction energy $\langle H_I \rangle$ shows larger fluctuations, but still much smaller than the subsystem energies, referred to as the "weak coupling" case.

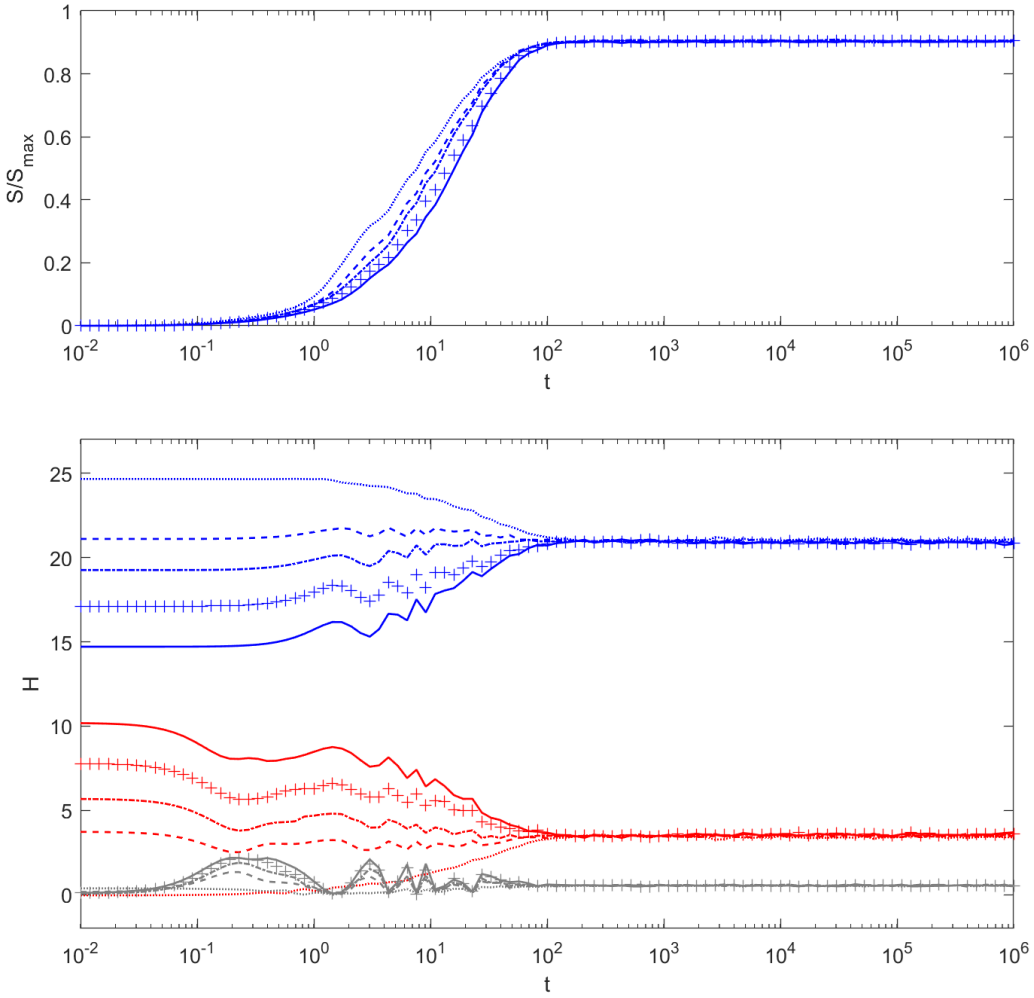


**Figure 8:** $E_I = 0.1$, different initial conditions converge to the same subsystem energy, reflecting the concept of "thermalization". Data: $\langle H_s \rangle$ (blue), $\langle H_e \rangle$ (red), $\langle H_I \rangle$ (gray), entropy $\dfrac{S}{S_{max}}$ (blue).

Figure 9 shows the case for $E_I = 1$. Under extremely strong coupling, the environment and the harmonic oscillator system are difficult to distinguish. Forcing a distinction between these two systems has no physical significance, and such a system has no corresponding physical reality; however, it eventually still reaches an equilibrium state of subsystem energy and entropy.

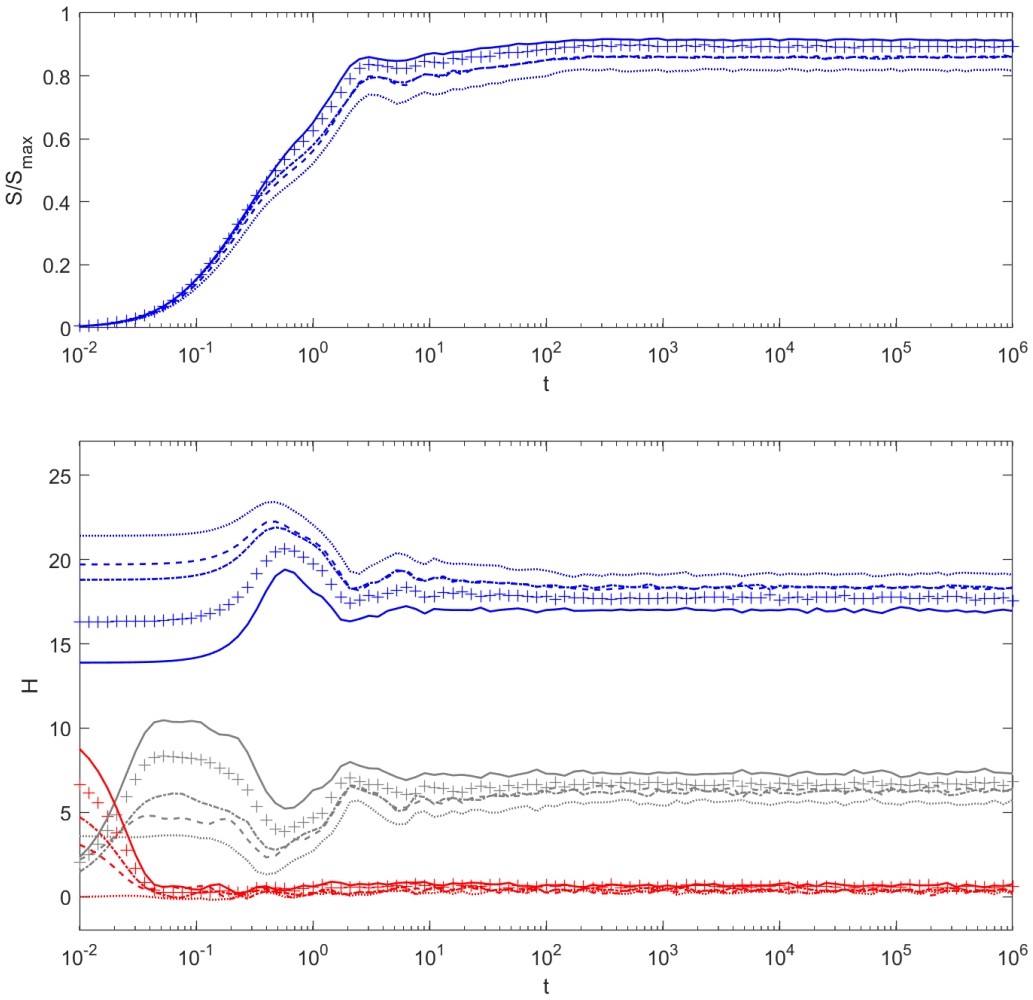


**Figure 9:** The case of $E_I = 1$, reflecting strong coupling, yet still showing equilibrium results. Data: $\langle H_s \rangle$ (blue), $\langle H_e \rangle$ (red), $\langle H_I \rangle$ (gray), entropy $\dfrac{S}{S_{max}}$ (blue).

### 3.5 Energy Distribution

Select the state corresponding to Figure 3 at different times ($E_I = 0.02$) and observe the eigenstate distribution of the harmonic oscillator at different times. To obtain the true energy distribution, the eigenstate energy density (number of eigenstates per unit energy) should also be given, yielding the results in Figure 10.

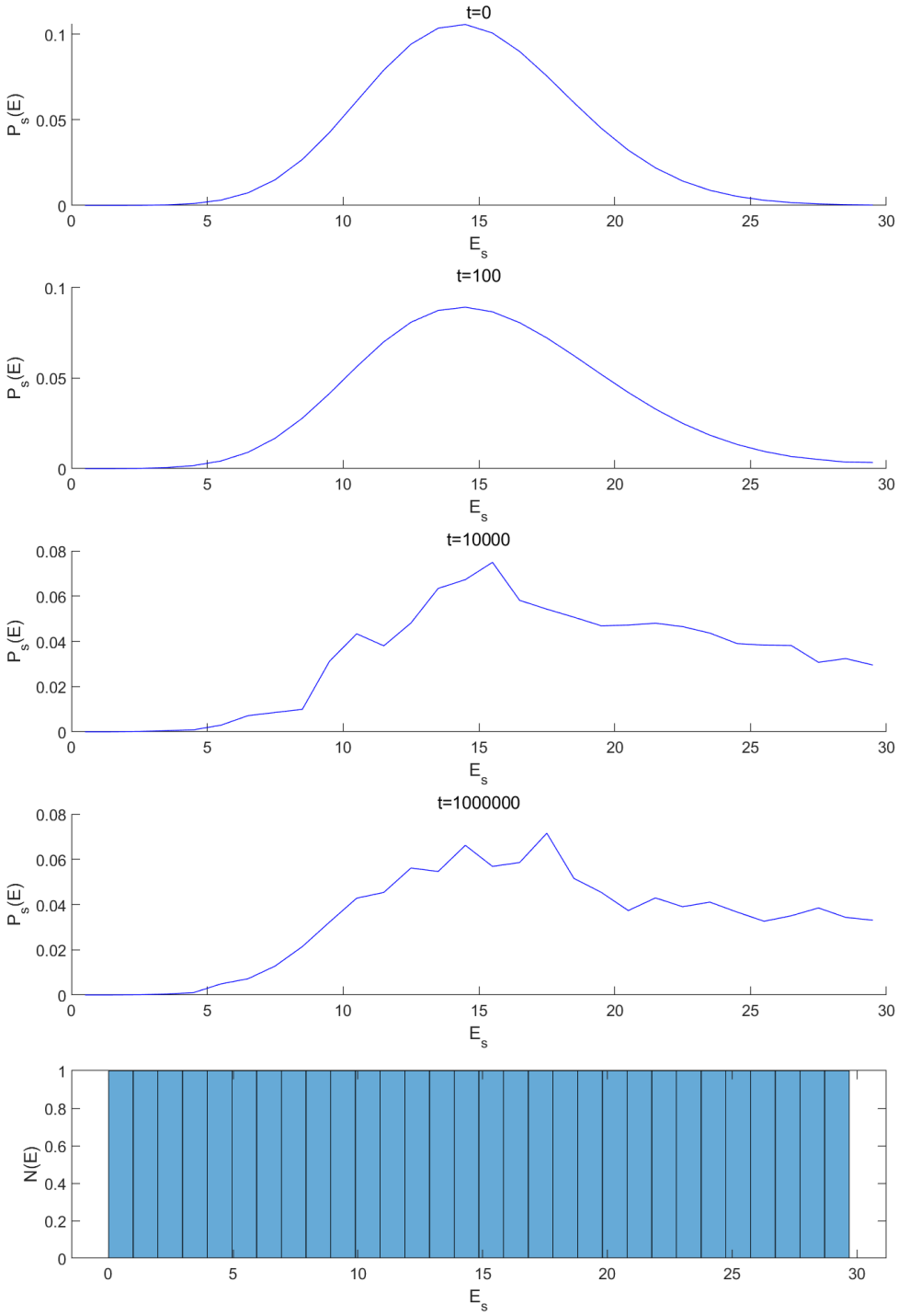


**Figure 10:** Harmonic oscillator energy distribution and its time evolution for the state corresponding to Figure 3, along with the density distribution of harmonic oscillator energy eigenstates (bottom).

Check the eigenstate distribution of the environment. Since there are too many eigenstates, change to statistical probability of energy within a certain interval, called binning processing. All subsequent distributions regarding the environment are processed with binning. The results in Figure 11 are obtained. The energy distribution tends to stabilize after a period of time.

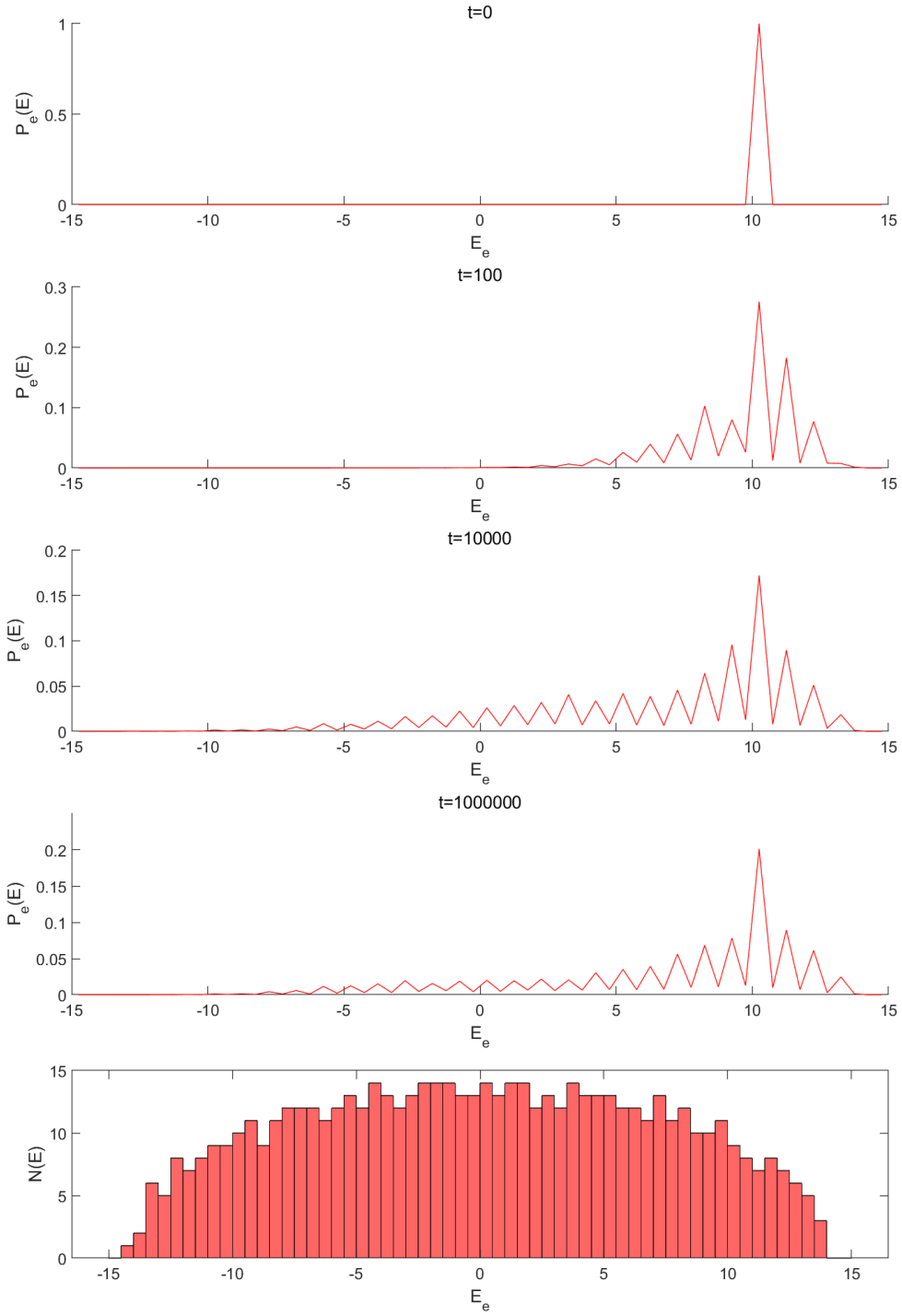


**Figure 11:** Environment energy distribution and its time evolution for the state corresponding to Figure 3, along with the density distribution of environment energy eigenstates (bottom). Data is processed with binning.

Examine the energy distribution of the stable state (taken at $t = 10^6$) under different initial states and different coupling strengths $E_I$, as shown in Figure 12 (harmonic oscillator) and Figure 13 (environment).

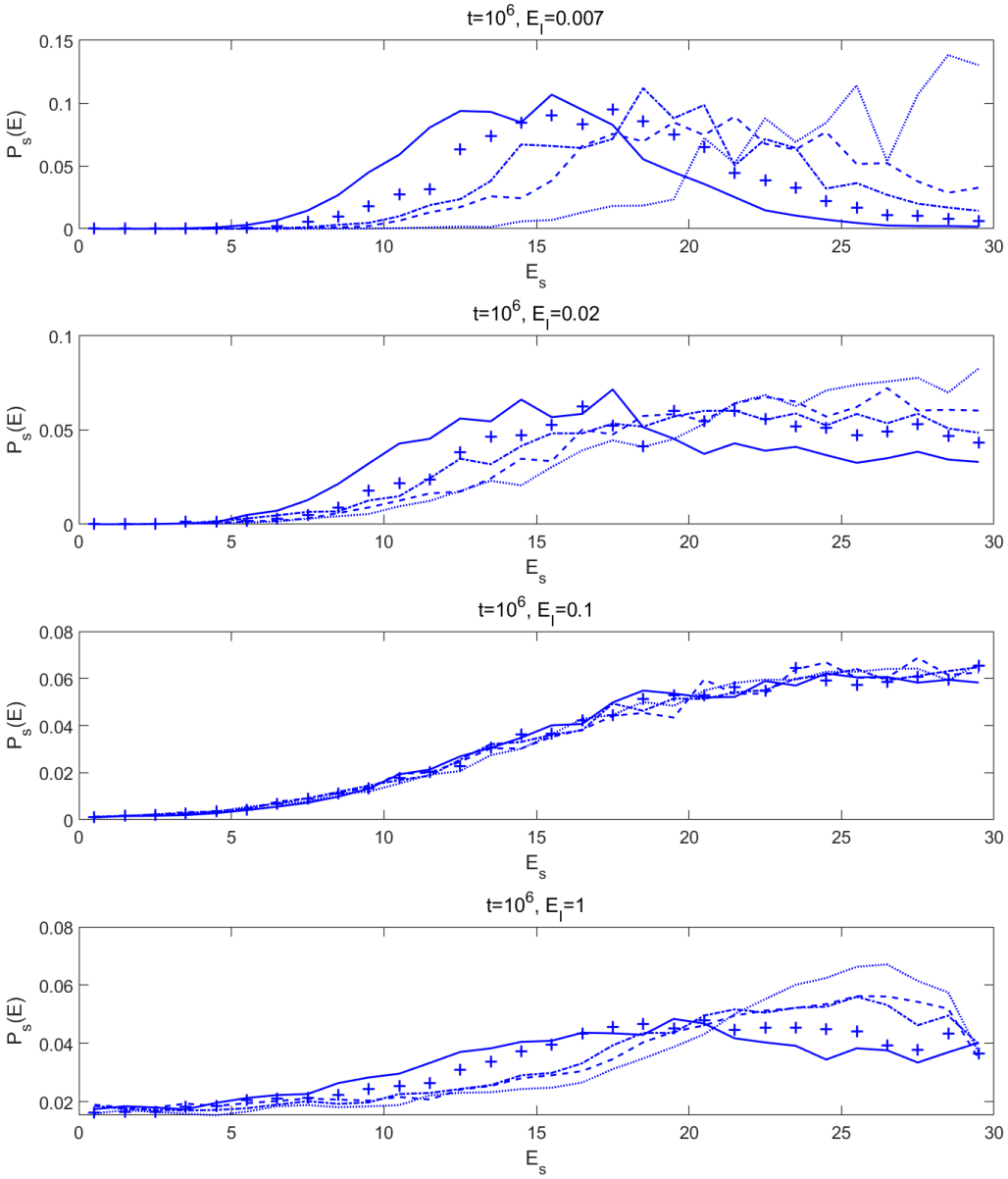


**Figure 12:** Harmonic oscillator energy distribution corresponding to different $E_I$ and different initial states at $t = 10^6$. When $E_I = 0.1$, different initial states finally converge to the same energy distribution.

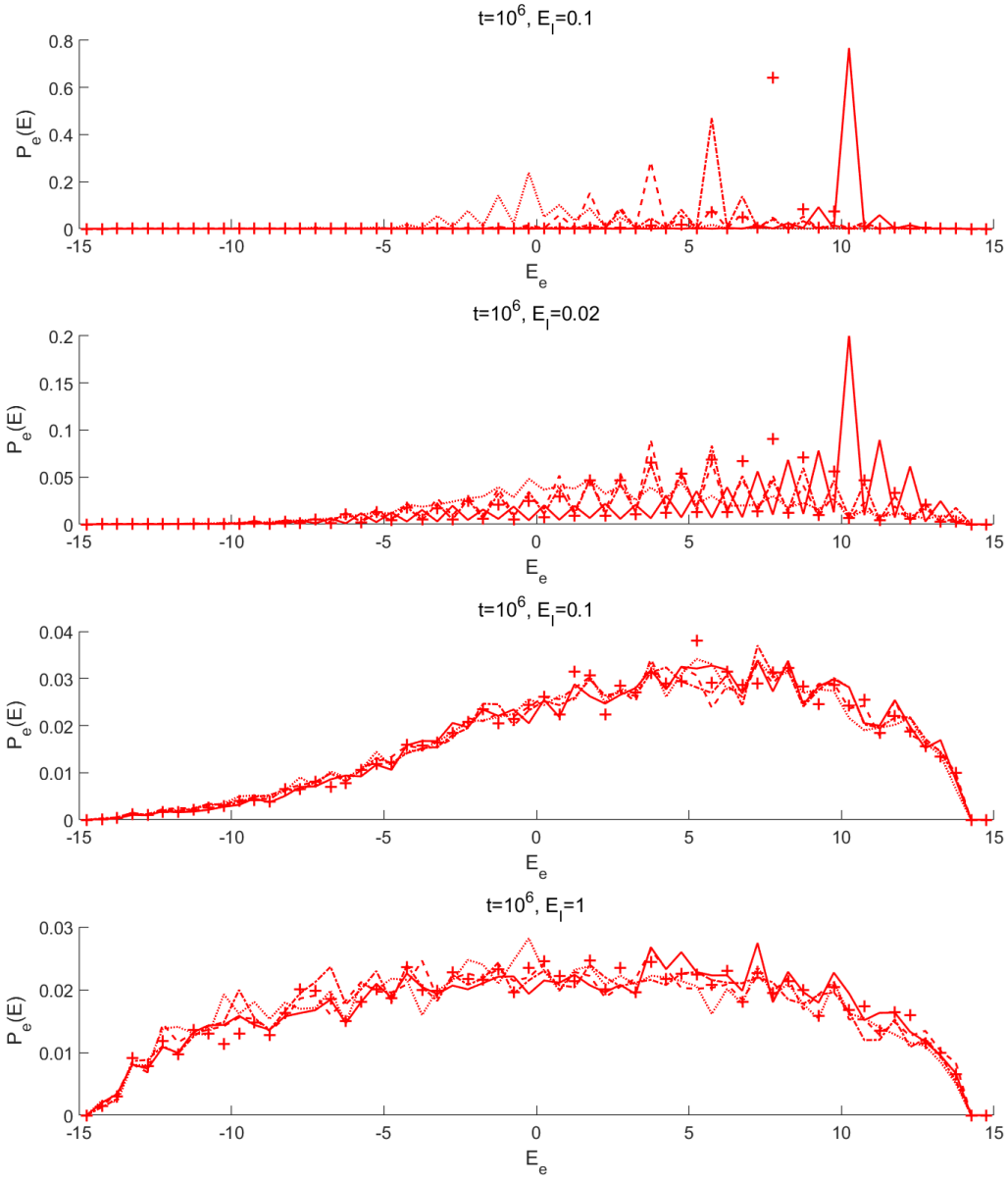


**Figure 13:** Environment energy distribution corresponding to different $E_I$ and different initial states at $t = 10^6$. When $E_I = 0.1$, different initial states finally converge to the same energy distribution.

In statistical physics, different subsystems in a "thermalized" state should have stable energy distributions. Only the case $E_I = 0.1$ in the above results satisfies this hypothesis, and its final state energy distribution is independent of the initial state, which is closer to real "thermalization". However, since the system does not have Gibbs-form energy (involving temperature), this is not a real thermodynamic system. Papers [1, 11] point out that if a "Generalized Canonical State" is considered, the idealized Gibbs energy can eliminate the small oscillations in the above calculation results.

## 3.6 Global Eigenvalues and Eigenstates

### 3.6.1 Energy Distribution in Subsystems

If $E_I = 0$, the eigenstates are the products of the eigenstates of the two subsystems, and the energy in the subsystem is distributed on only one value. Using the method in Section 3.5 to solve for the distribution in the subsystem, information on eigenstate "slices" can be given. Figure 14 and Figure 15 show the subsystem (harmonic oscillator and environment, respectively) energy distributions for different $H_w$ eigenstates ($E_I = 0.007$).

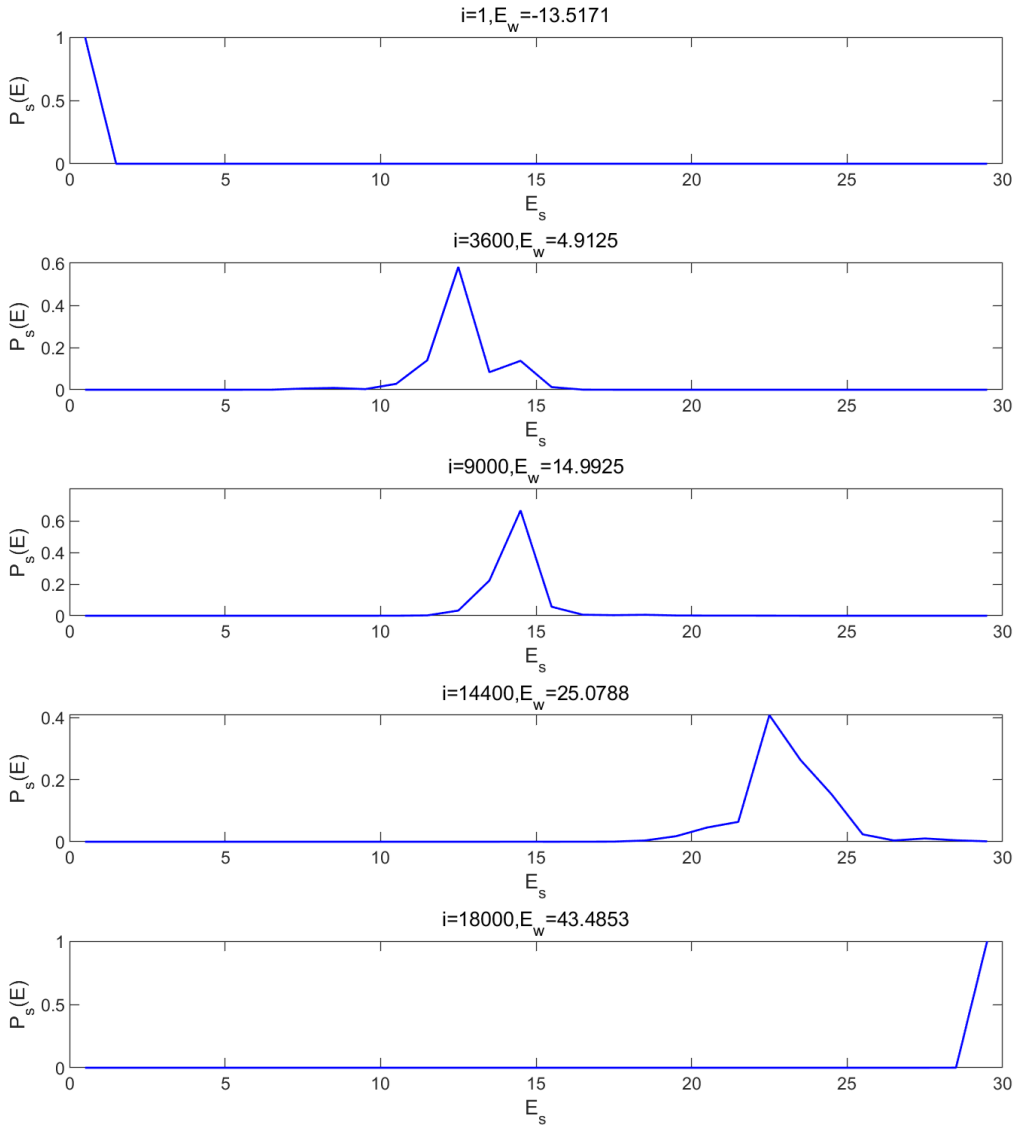


**Figure 14:** Distribution of some $H_w$ eigenstates in the harmonic oscillator subspace under $E_I = 0.007$. The result approximates a delta function with extremely small broadening.

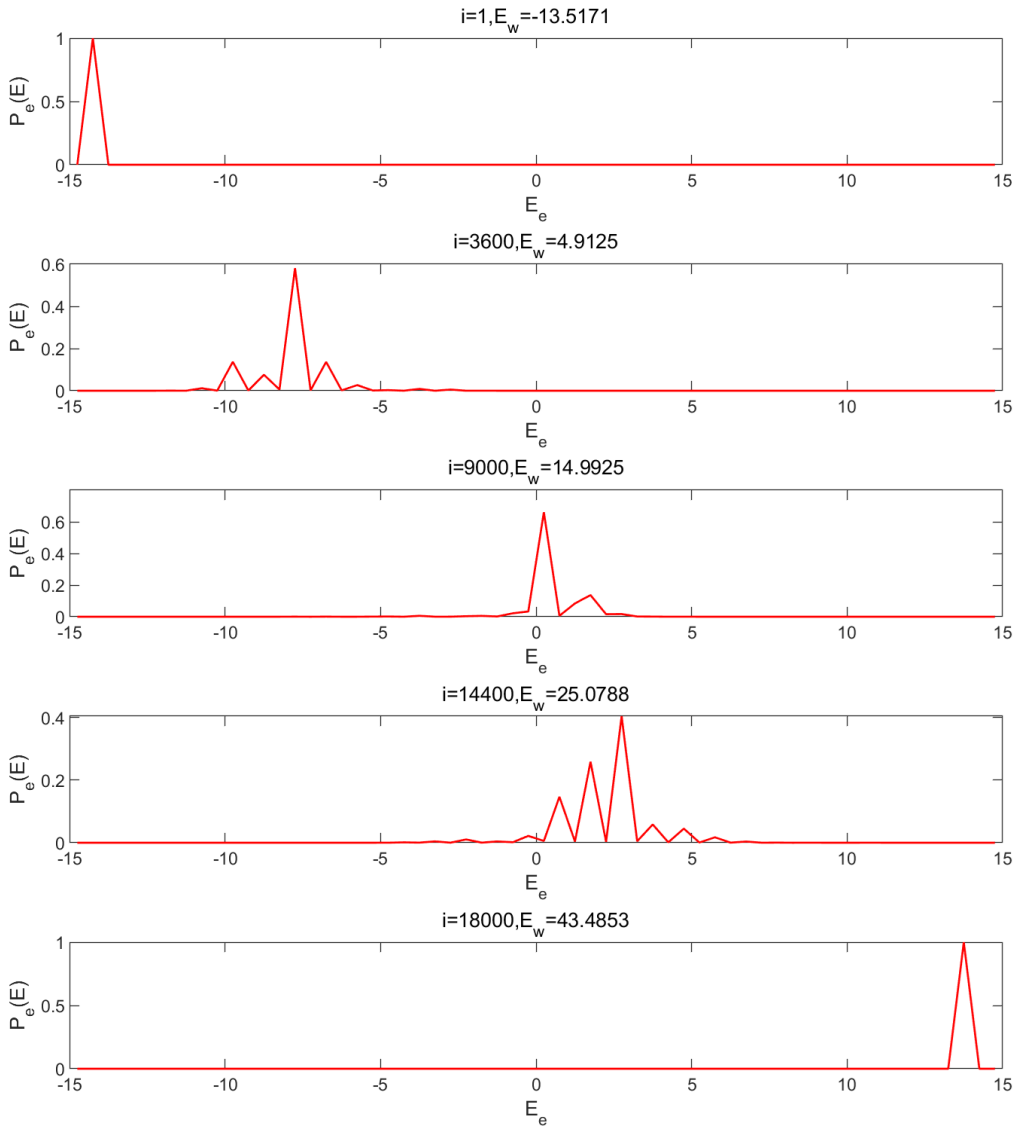


**Figure 15:** Distribution of some $H_w$ eigenstates in the environment subspace under $E_I = 0.007$. The result approximates a delta function with extremely small broadening.

This result is very close to the $E_I = 0$ case. Although the energy distribution is not just on a single subsystem eigenstate, it still possesses significant localization properties, indicating weak coupling. Figure 16 shows the subspace energy distribution of three adjacent states ($E_I = 0.007$). Although the difference in global energy of these states is very small, the energy distributions are vastly different, illustrating that states with the same total energy can have distinct and rich structures.

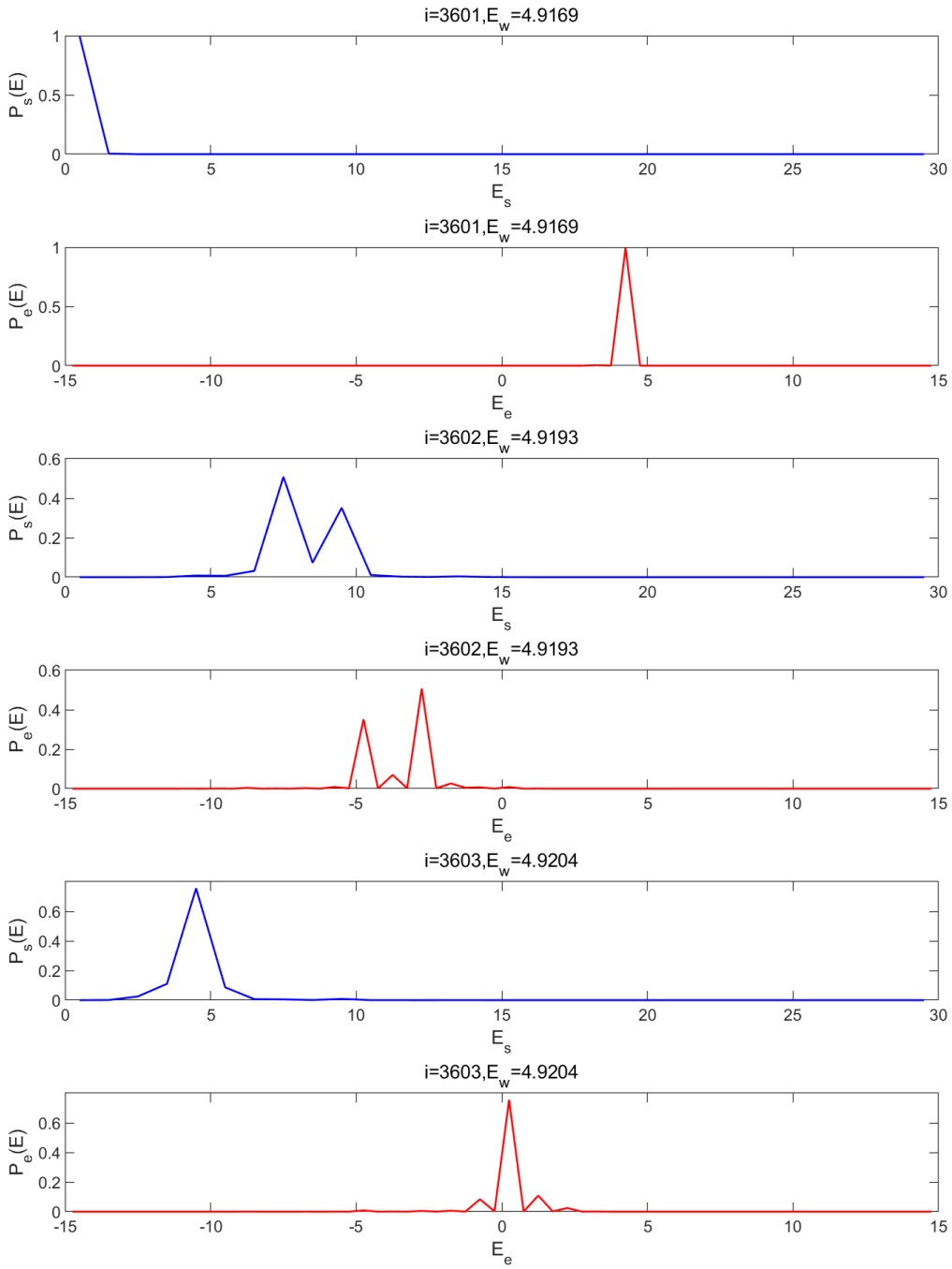


**Figure 16:** Distribution of three adjacent $H_w$ eigenstates in two subspaces under $E_I = 0.007$. Despite energies being very close, the eigenstates are vastly different.

Similarly, taking $E_I = 0.1$, the results obtained are shown in Figure 17 (harmonic oscillator subspace), Figure 18 (environment subspace), and Figure 19 (adjacent energy eigenstates). When $E_I = 0.1$, there is "weak coupling" between the system and the environment, but the coupling strength is sufficient to mix the eigenstates of the harmonic oscillator and the environment; comparing with Figure 14, the difference in energy distribution between adjacent eigenstates becomes even smaller.

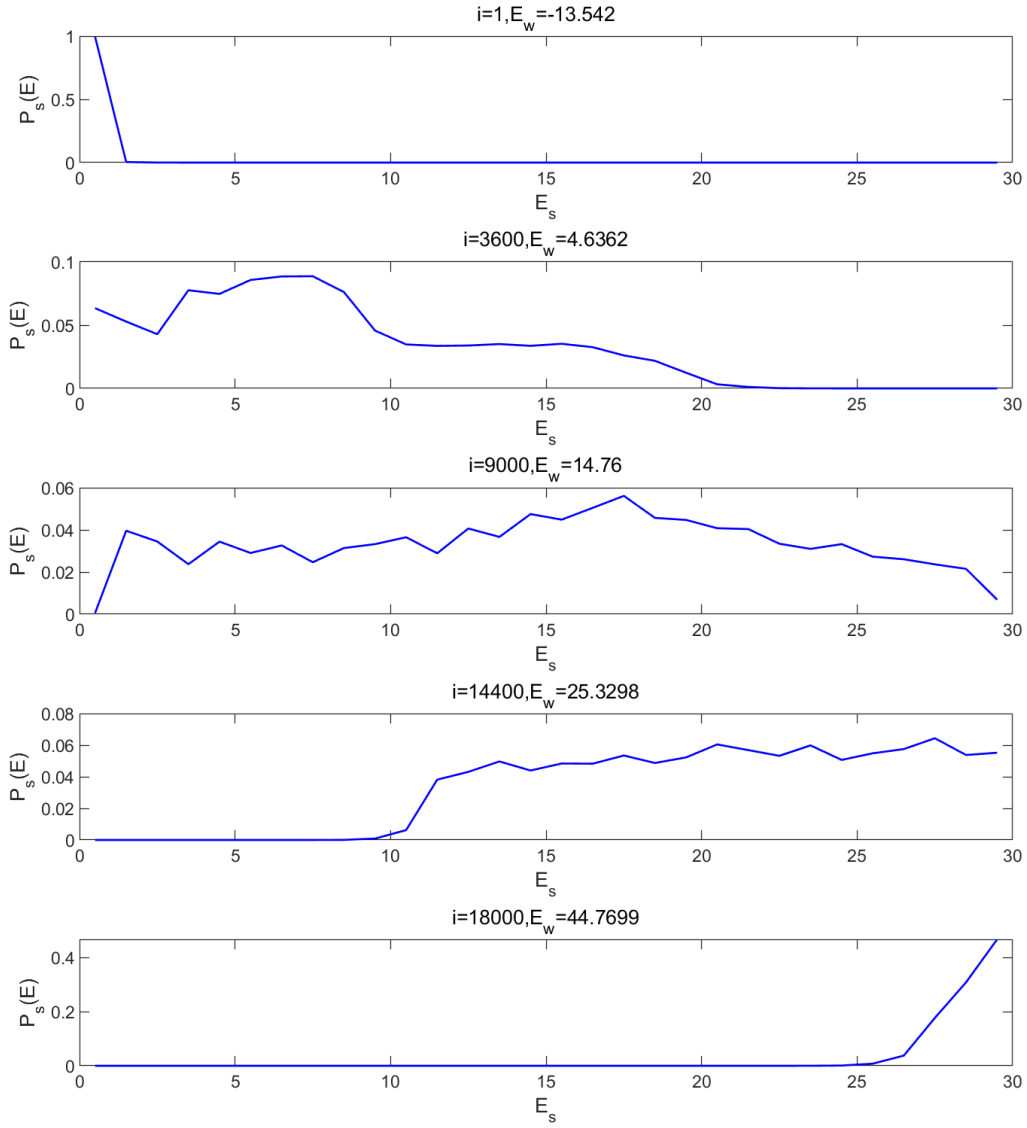


**Figure 17:** Distribution of some $H_w$ eigenstates in the harmonic oscillator subspace under $E_I = 0.1$. Due to stronger inter-subsystem coupling, the energy broadening is larger compared to above.

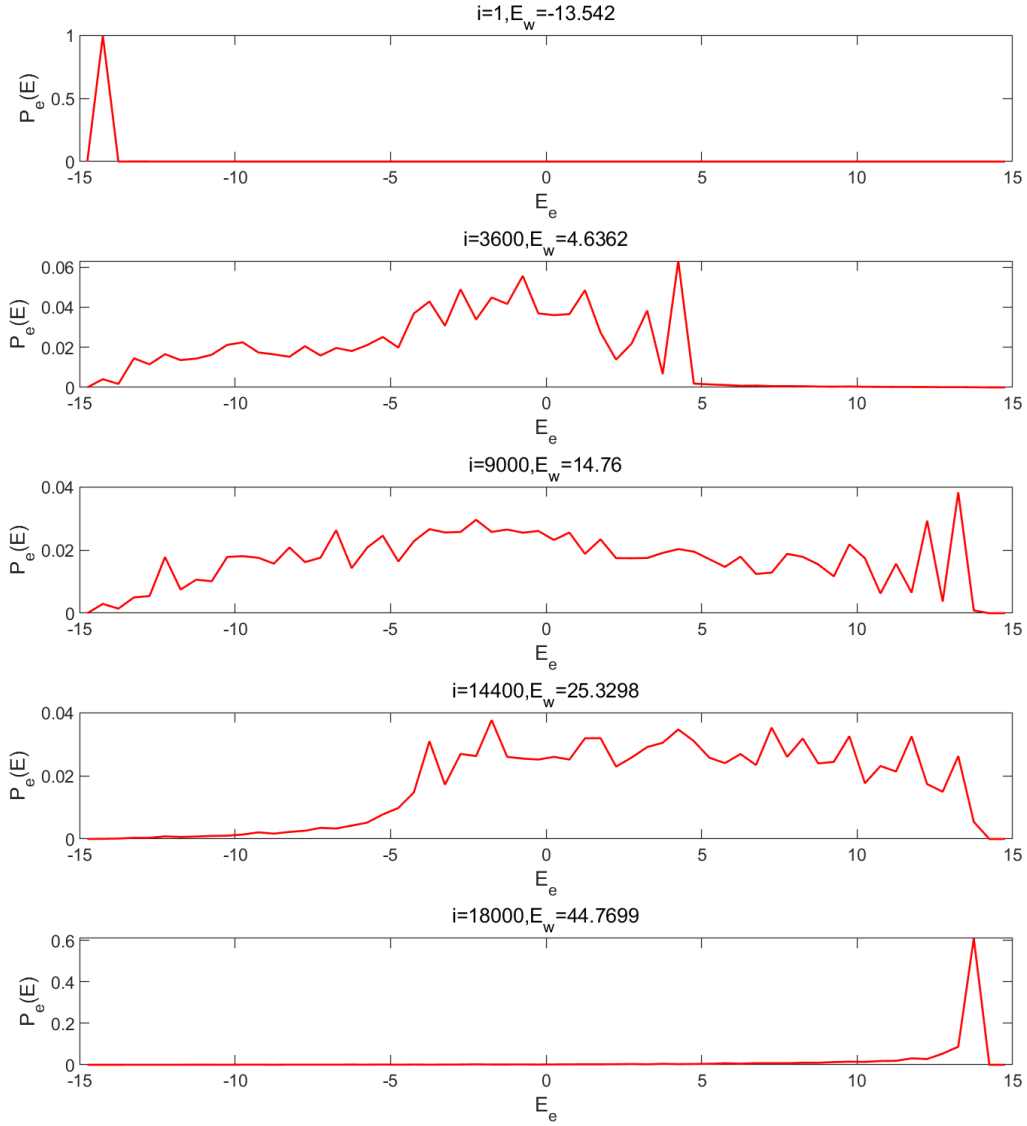


**Figure 18:** Distribution of some $H_w$ eigenstates in the environment subspace under $E_I = 0.1$. Due to stronger inter-subsystem coupling, the energy broadening is larger compared to above.

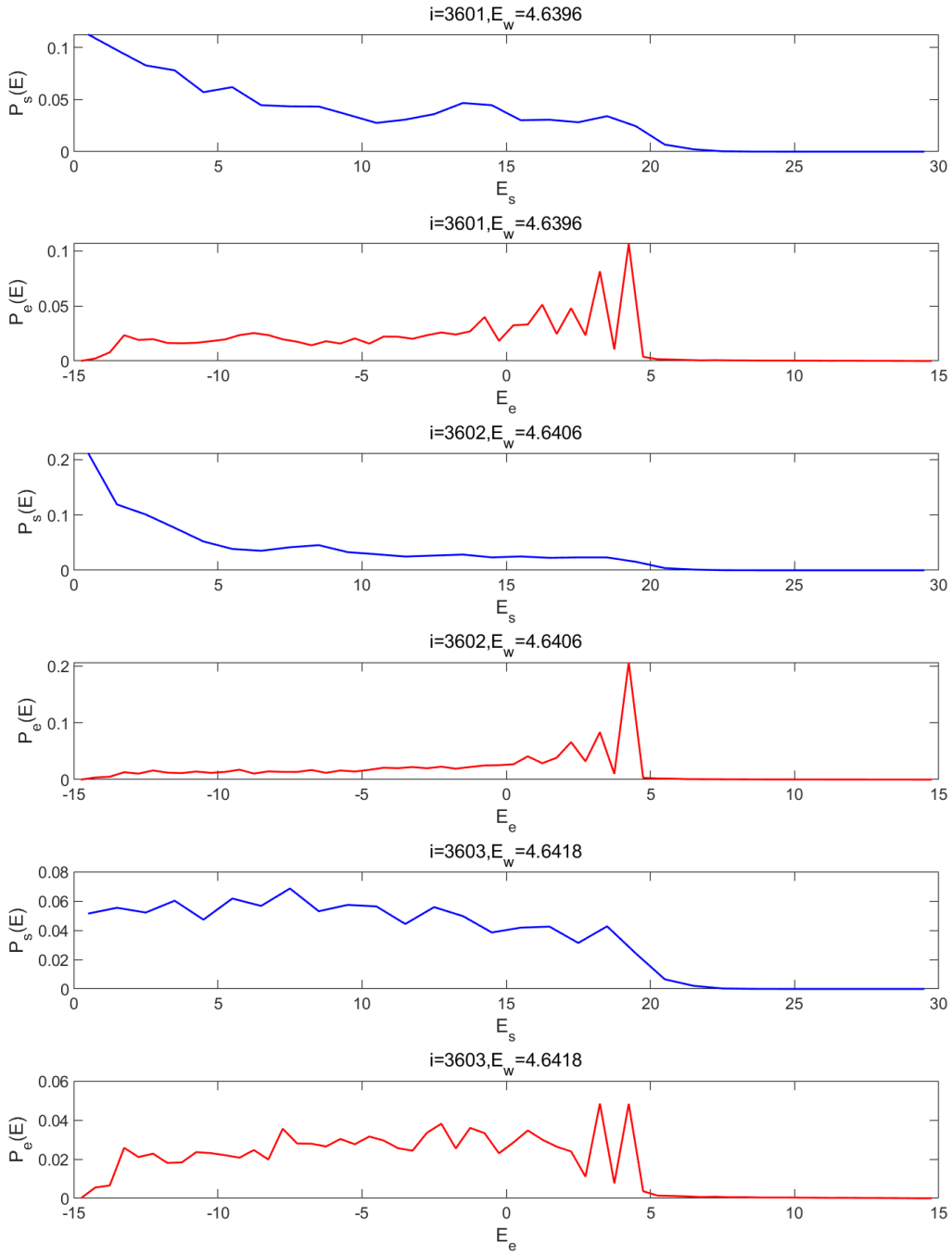


**Figure 19:** Distribution of three adjacent $H_w$ eigenstates in two subspaces under $E_I = 0.1$. Due to larger energy broadening, the distinction between adjacent eigenstates becomes smaller.

### 3.6.2 Energy Distribution in Global Space

Define the global density matrix $\rho_w = |\psi\rangle_w \langle\psi|_w$, and the probability distribution of eigenenergies $P_w(E) = diag(\rho_w^E)$. Below, the global energy eigenstate distributions of the initial states generated according to the method in Section 2.2.3 under different $E_I$ are given, yielding the results in Figure 20.

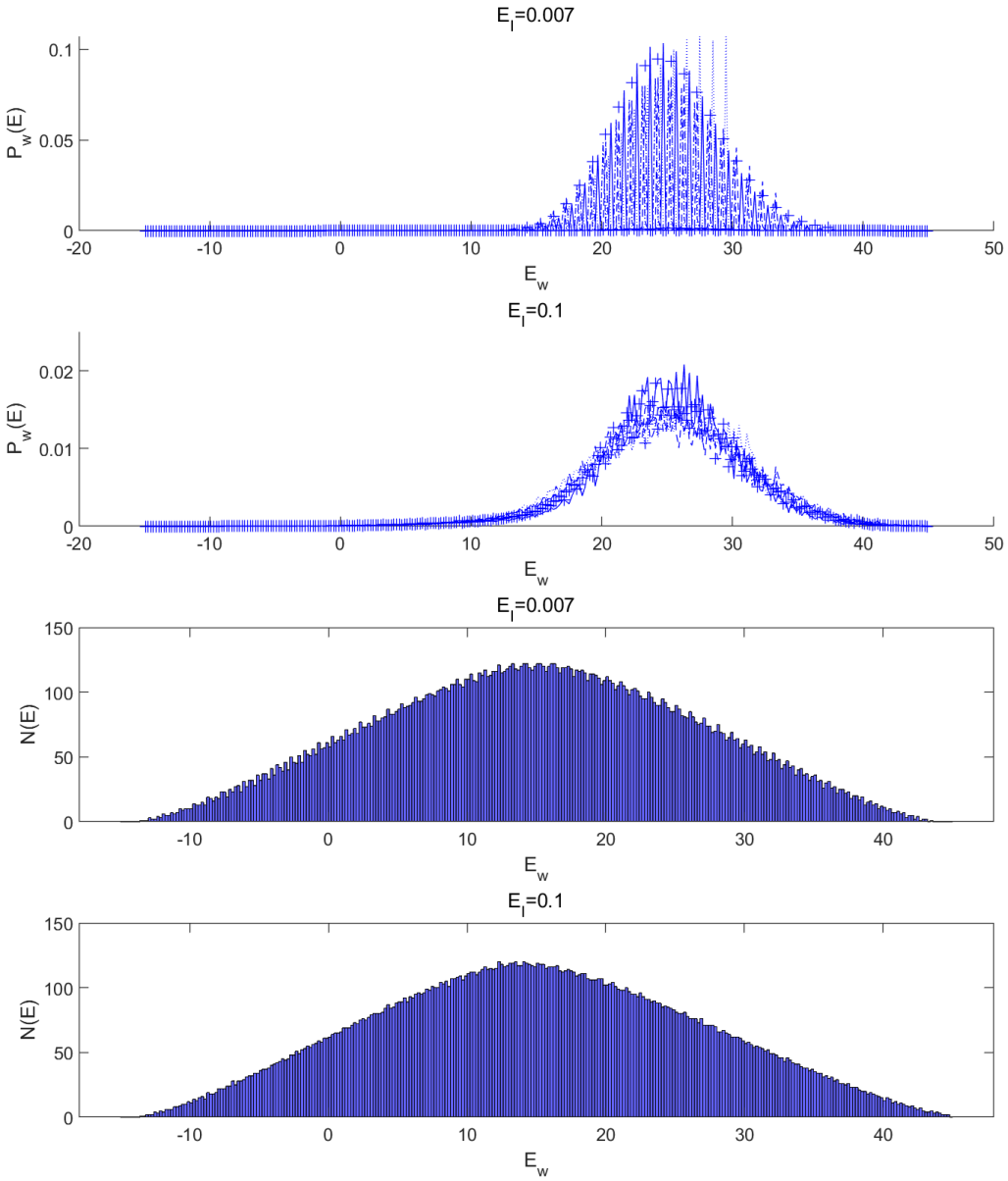


**Figure 20:** Global energy eigenstate distributions for five initial states, taking $E_I$ as 0.007 and 0.1 respectively, with data processed by binning; meanwhile, histograms of eigenstate density are given, where it can be seen that the eigenstate distribution has almost no relation to $E_I$.

Figure 21 shows the detailed parts of Figure 20. The $E_I = 0.007$ curve has huge oscillations, and different initial states are vastly different.

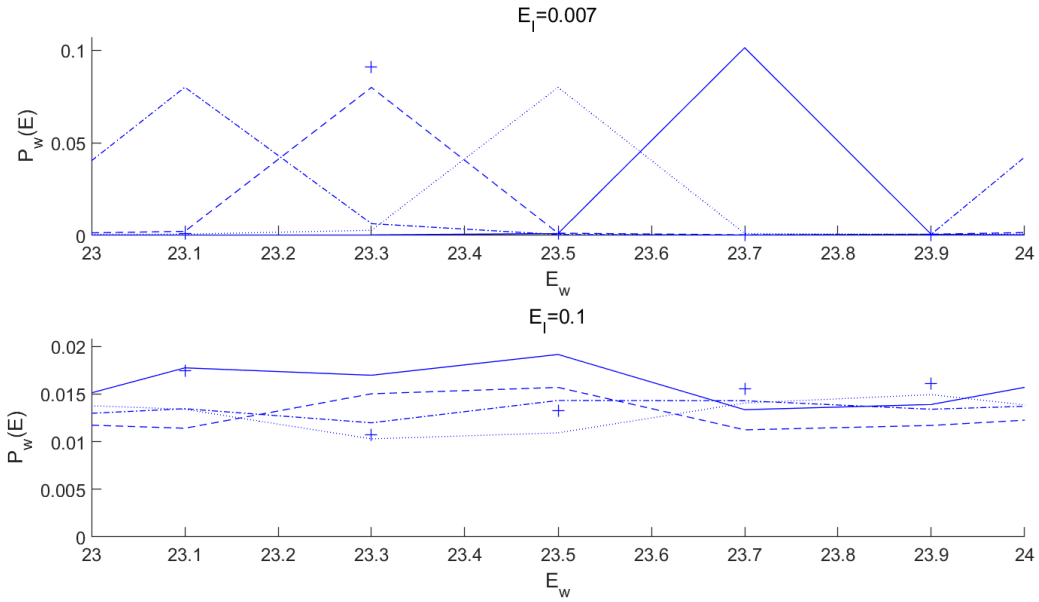


**Figure 21:** Local magnification of the first two plots in Figure 20. The curve for $E_I = 0.007$ frequently hits 0, while the $E_I = 0.1$ curve does not; meanwhile, the extreme points and near-zero points for different initial states with $E_I = 0.007$ are vastly different.

Consider the uncoupled limit $E_I = 0$. The product of subsystem eigenstates $|n\rangle_s |i\rangle_e$ is the global eigenstate, meaning $|n\rangle_s |i\rangle_e$ can be viewed as a delta function under the $H_w$ eigenstate decomposition (distributed on only one global eigenstate). Then for $E_I = 0.007$, if there exists a k-th global eigenstate $|E_k\rangle$ that has a large overlap with it ("overlap" in paper [1] refers to the modulus of $\langle E_k| |n\rangle_s |i\rangle_e$), then the degree of overlap of adjacent global eigenstates will be much smaller (the modulus of $\langle E_{k+1}| |n\rangle_s |i\rangle_e$ is much smaller). However, in the case of $E_I = 0.1$, the energy distribution of adjacent eigenstates in the subsystem will not change much (because energies are close), indicating that the overlap of energy will be smoother (meaning the difference between $\langle E_k| |n\rangle_s |i\rangle_e$ and $\langle E_{k+1}| |n\rangle_s |i\rangle_e$ is smaller).

Similarly, when $E_I = 0.1$, the broad energy distribution of eigenstates in the subsystem indicates that although the energy distribution of two initial states in the subspace may be different, they are still similar in the total energy distribution (as shown in Figure 20, the total energy is fixed at 25). Furthermore, since the density matrix plus phase can completely define a state, under equilibrium conditions (refer to Section 3.1, phases are randomly distributed), the density distribution $P_w(E)$ has no relation to the initial phase, and similar subsystem density distributions $P_s(E)$ and $P_e(E)$ can also be given.

Since the initial state is the product of a coherent state and an environment subsystem eigenstate, where although the coherent state is not an energy eigenstate of the harmonic oscillator, it possesses certain localization (Note: its density distribution is $P_s(E_n) = e^{-\overline{\alpha}\alpha}\frac{(\overline{\alpha}\alpha)^n}{n!}$, $E_n = (n + \frac{1}{2})\hbar\omega = n + \frac{1}{2}$, with a peak around $n = \overline{\alpha}\alpha$, and then gradually decaying, presenting a structure of first rising and then falling as $n$ increases (when $|\alpha| > 1$, otherwise strictly decreasing), having certain localization), it

basically conforms to the above discussion.

If similar calculations are performed in larger systems, paper [10] points out the existence of a "quantum limit", where even at $E_I = 0.1$, the global energy distribution may become a series of sharp peaks (see Figure 21). Only within certain limits will the smooth energy distribution under $E_I = 0.1$ appear, which reflects the difference between classical statistical mechanics and quantum statistical mechanics.

$E_I = 0.007$ reflects another limit, where $P_w(E)$ is more jagged, inconsistent with classical statistical properties. To some extent, this reflects that $E_I = 0.1$ is the main factor for the "thermalization" behavior of larger systems; while $E_I = 0.007$ reflects a localized, non-thermalizing system (called "Many-Body Localization", reference [9]), which cannot fully connect energy levels that allow exchange energetically (e.g., some states with the same/approximate total energy but different subsystem energies). However, such localized situations reflect additional conserved quantities by comparison, although compared to the $E_I = 0$ limit, symmetry is partially broken, making $\langle H_s \rangle, \langle H_e \rangle$ no longer conserved quantities.

### 3.6.3 Effective Dimension

According to the content of Section 2.1.3, the effective dimensions corresponding to different initial states under different $E_I$ can be calculated, as shown in Table 1:

**Table 1:** Effective dimensions $d^w_{eff,i}, i = 1,2,3,4,5$ and their average value $d^w_{eff}$ ($d^w_{eff}$, Eq. 5) for the five distributed initial states under different $E_I$. If $P_w(E)$ is broader and smoother, the effective dimension is larger; for example, the effective dimension of the initial state corresponding to $E_I = 0.1$ is much larger than that of $E_I = 0.007$ (see Figure 20 and Figure 21). The table also gives the standard deviation $\sigma^w_{eff}$ of the results for different initial states and its ratio $\Delta$, as well as the percentage of the mean relative to the maximum case ($E_I = 0.1$).

| $E_I$ | $d^w_{eff,1}$ | $d^w_{eff,2}$ | $d^w_{eff,3}$ | $d^w_{eff,4}$ | $d^w_{eff,5}$ | $d^w_{eff}$ | $\sigma^w_{eff}$ | $\Delta$ | $\frac{d^w_{eff}}{d^w_{eff}\vert_{E_I=0.1}}$ |
|---|---|---|---|---|---|---|---|---|---|
| 1 | 1296.17 | 1785.94 | 1705.88 | 2441.92 | 2782.81 | 2002.54 | 599.11 | 29.92% | 53.96% |
| 0.1 | 3859.35 | 3933.42 | 3974.40 | 3635.24 | 3152.24 | 3710.93 | 386.78 | 9.13% | 100.00% |
| 0.02 | 759.02 | 805.19 | 583.79 | 349.72 | 110.67 | 521.68 | 291.15 | 55.81% | 14.06% |
| 0.007 | 50.43 | 101.61 | 40.80 | 23.39 | 17.66 | 46.78 | 33.36 | 71.30% | 1.26% |

The different behaviors of eigenstates for $E_I = 0.1$ and $E_I = 0.007$ can be clearly described by $d^w_{eff}$. The standard deviation ratio $\Delta$ can also measure the behavior of "scattering", where it is smallest when $E_I = 0.1$, consistent with the previous discussion.

### 3.7 Variations in Parameters and Initial States

From the previous discussion, it is known that to achieve the "thermalization" effect, the value of $E_I$ needs to be within a certain range. However, for larger systems, "thermalization" should be more trivial, while "non-thermalization" behavior requires specific parameter values. Since the ACL model is too simple (though computationally expensive), more conclusions regarding initial parameter adjustments cannot be given.

The previous text discussed the impact of the initial state on equilibrium, but the initial state was a carefully designed product of a coherent state and an environmental eigenstate. In the actual physical world, there exist initial states with very low entropy (the one described above is also one, because its environment part is an eigenstate), although this is generally not the case. Paper [1] points out that low-entropy initial states are often related to the "fine-tuning problem" in cosmology.

### 3.8 Eigenstate Thermalization Hypothesis (ETH)

The concept of "Eigenstate Thermalization" was first proposed by Mark Srednicki in 1994 [12], aiming to explain when and why equilibrium statistical mechanics can accurately describe isolated quantum mechanical systems, dedicated to understanding how systems initially prepared far from equilibrium evolve in time to seemingly reach a state of thermal equilibrium [8]. It suggests that thermalizing systems can be understood using the eigenstates of the global Hamiltonian. The comparison between Figure 16 and Figure 19 can also to some extent show that in the case of $E_I = 0.1$, the energy distributions of global eigenstates on the subsystem are more similar. This indicates that in the "thermalization" under the $E_I = 0.1$ case, the energy distribution of the subsystem is the sum of individual global eigenstate distributions, which are all very similar, reflecting signs of the Eigenstate Thermalization Hypothesis. Figure 22 shows the similarity between the subsystem energy distributions of some global eigenstates and those in Figure 12 and Figure 13, but the differences between the two indicate that ETH is not fully manifested in this system.

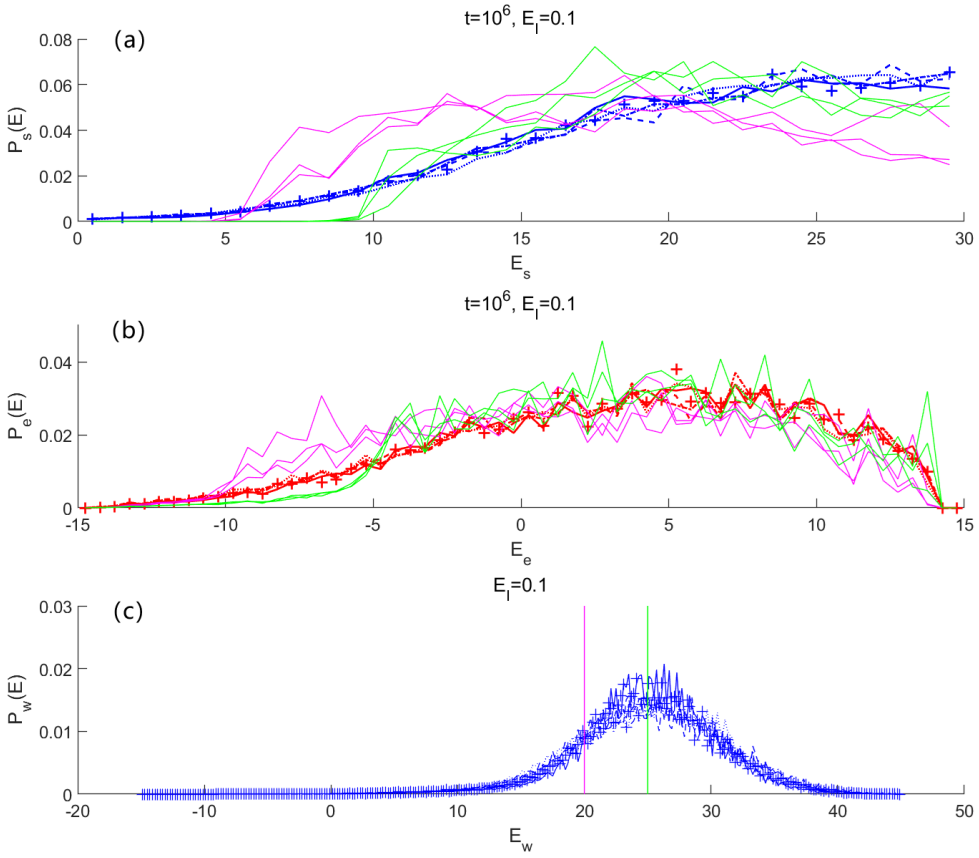


**Figure 22:** Verification of the Eigenstate Thermalization Hypothesis ($E_I = 0.1$). Subsystem energy distributions of the initial state (Figure 12 and Figure 13, taking $t = 10^6$ for equilibrium) and subsystem energy distributions of several global energy eigenstates: (a) Harmonic oscillator; (b) Environment. (c) Selection of eigenstates: Since the initial state energy is 25, eigenstates near global energy 20 (pink lines) and 25 (green lines) are selected, three of each (corresponding to the three pink lines and three green lines in (a) and (b) above). Actual energies are between $(20 \pm 0.0020)$ and $(25 \pm 0.0031)$, with errors on the order of $0.01\%$.

# 4 Conclusion

This paper systematically investigated the equilibration process of the ACL model and obtained the phenomenon of dephasing during the equilibration process. Dephasing allows equilibration to occur in the absence of thermodynamic temperature. Although the concept of thermodynamic temperature does not apply to this system, the system still exhibited the phenomenon of "thermalization", i.e., different initial states eventually evolved to reach the same subsystem energy distribution. When thermalization holds, the global energy distribution is smooth (Figure 20, $E_I = 0.1$); when thermalization does not hold, the total energy distribution is jagged (Figure 21, $E_I = 0.007$). Such behavior is related to the intrinsic characteristics of total energy eigenstates; a smooth energy distribution is related to ergodicity, and a limit exists in larger systems. This phenomenon is related to the existence and absence of thermalization in actual condensed matter systems.

Although the ACL model is very simple, it can still reflect certain factors of equilibrium; due to the small scale and some non-physical reasons, some factors cannot be demonstrated. Understanding some behaviors of the ACL system is useful for exploring the selection effects of physical laws [13] and can also help us understand the real physical world.

# 5 Relation to the Course (Fundamental Theory)

## 5.1 ZCL Model (referred to as Caldeira-Leggett Model in this paper)

Robert Zwanzig first proposed the Zwanzig Hamiltonian in the field of statistical physics in 1973 [14]. Later, A.O. Caldeira and A.J. Leggett proposed the Caldeira-Leggett model (whose Hamiltonian is the same as the Zwanzig Hamiltonian) in two papers published in 1983 [6, 7] to explain Brownian motion.

The ZCL model replaces the environment with oscillators. A particle is coupled to many harmonic oscillators and is located in a potential field. The Hamiltonian is given by Eq. 1. If the interaction between this particle and each environmental particle is equivalent to connecting them with a spring, and there is no interaction between environmental particles, then the Hamiltonian can be written in the following simplified form:

$$H = \frac{p^2}{2m} + V(x) + \sum_j \left[ \frac{p_x^2}{2m_j} + \frac{1}{2} k_j (q_j - x)^2 \right] \tag{8}$$

The Hamilton's equations of motion are:

$$\begin{cases} \dfrac{dx}{dt} = \dfrac{p}{m}, & \dfrac{dp}{dt} = -\dfrac{dv}{dx} + \sum_j k_j (q_j - x) \\ \dfrac{dq_j}{dt} = \dfrac{p_j}{m_j}, & \dfrac{dp_j}{dt} = -k_j (q_j - x) \end{cases}$$

Solving this yields the equation of motion for the central particle:

$$m\frac{d^2}{dx^2} + \int_0^t B(t - t') \frac{dx}{dt}(t') dt' + V' + B(t) x(0) = \xi(t)$$

where:

$$\begin{cases} B(t) = \sum_j k_j \cos(\omega_j t) \\ \xi(t) = \sum_j (q_j(0) k_j \cos(\omega_j t) + p_j(0) \sin(\omega_j t)) \end{cases}$$

Considering random $\omega_j$ and $k_j$, $B(t)$ can be approximated as a $\delta$ function. If the $\omega$ distribution is $dN = N(\omega) d\omega$, corresponding to stiffness coefficient $k(\omega)$, then when

$$N(\omega) k(\omega) = \frac{2\gamma}{\pi}$$

we have

$$B(t) = \int_0^\infty N(\omega) k(\omega) \cos(\omega t) d\omega = \gamma \delta(t)$$

The equation of motion becomes:

$$m\frac{d^2}{dx^2} + \gamma \frac{dx}{dt} + V' = \xi(t) (t \neq 0) \tag{9}$$

This is identical to the Langevin equation, reflecting Brownian motion. For random $\omega_j$ and $k_j$, $\xi(t)$ is also random; if the equipartition theorem holds for the initial states $q_j(0), p_j(0)$, then we can also approximately obtain

$$\mathbb{E}(\xi(t)\xi(s)) \to \gamma k_B T \delta(t-s)$$

The conditions are the same as above.

## 5.2 Simple Harmonic Oscillator (SHO) Model

The classical harmonic oscillator Hamiltonian is $H = \dfrac{p^2}{2m} + \frac{1}{2}m\omega^2$. The harmonic oscillator in quantum mechanics uses the same Hamiltonian, but the momentum operator is $p = -i\hbar\dfrac{d}{dx}$. Then the time-independent Schrödinger equation is:

$$\left(-\frac{\hbar^2}{2m}\frac{d^2}{dx^2} + \frac{1}{2}m\omega^2\right)\psi(x) = E\psi(x)$$

The solution to the equation needs to be expressed using Hermite polynomials:

$$\begin{cases} \psi_n(x) = \dfrac{1}{\sqrt{2^n n!}}\left(\dfrac{m\omega}{\pi\hbar}\right)^{\frac{1}{4}} \exp\left(-\dfrac{m\omega x^2}{2\hbar}\right) H_n\left(\sqrt{\dfrac{m\omega}{\hbar}}x\right) \\ E_n = (n+\frac{1}{2})\hbar\omega \end{cases} \tag{10}$$

where $H_n(x) = (-1)^n e^{x^2}\frac{d^n}{dx^n}e^{-x^2}$. A better way to describe the eigenstates $|n\rangle$ and the relationships between them is to use ladder operators (called creation and annihilation operators in second quantization scenarios), defined as:

$$a = \sqrt{\frac{m\omega}{2\hbar}}x + i\frac{p}{\sqrt{2m\hbar\omega}}, \qquad a^\dagger = \sqrt{\frac{m\omega}{2\hbar}}x - i\frac{p}{\sqrt{2m\hbar\omega}} \tag{11}$$

Then:

$$a^\dagger a\,|n\rangle = n\,|n\rangle\,, a^\dagger\,|n\rangle = \sqrt{n+1}\,|n+1\rangle$$
$$a\,|n\rangle = \sqrt{n}\,|n-1\rangle\,, a\,|0\rangle = 0\,|\rangle$$

Also (Note: $px - xp = -i\hbar$):

$$H = \hbar\omega\left(a^\dagger a + \frac{1}{2}\right), \qquad [a, a^\dagger] = aa^\dagger - a^\dagger a = 1 \tag{12}$$

### 5.2.1 Coherent States

Coherent states are the quantum description of classical simple harmonic oscillation. The aforementioned harmonic oscillator eigenstates only reflect energy (or amplitude in the classical case) characteristics, not phase or time evolution characteristics. Although the content of coherent states was not covered in the quantum mechanics course, since the derivation of various properties basically does not depart from the knowledge of the quantum mechanics course (normalization, harmonic oscillator states,

matrix element calculation, etc.), it is placed in this section. One definition of a coherent state is:

$$|\alpha\rangle = e^{-\frac{1}{2}\overline{\alpha}\alpha}\sum_{n=0}^{\infty}\frac{\alpha^n}{\sqrt{n!}}|n\rangle \tag{13}$$

Note that $\sum_{n=0}^{\infty}\left|e^{-\frac{1}{2}\overline{\alpha}\alpha}\left(\frac{\alpha^n}{\sqrt{n!}}\right)\right|^2 = e^{-\overline{\alpha}\alpha}\sum_{n=0}^{\infty}\frac{(\overline{\alpha}\alpha)^n}{n!} = e^{-|\alpha|^2}e^{|\alpha|^2} = 1$, indicating the state is normalized.

Since $|n\rangle = \frac{(a^\dagger)^n}{\sqrt{n!}}|0\rangle$, the above equation can be expanded as:

$$|\alpha\rangle = e^{-\frac{1}{2}\overline{\alpha}\alpha}\sum_{n=0}^{\infty}\frac{\alpha^n(a^\dagger)^n}{n!}|0\rangle = e^{-\frac{1}{2}\overline{\alpha}\alpha}e^{\alpha a^\dagger}|0\rangle = e^{\alpha a^\dagger - \overline{\alpha}a}|0\rangle \tag{14}$$

This yields the form of the coherent state given in Appendix A of paper [1]. The proof of the last equality is seen in Section 5.2.2.

Coherent states have the following properties:

- The coherent state is an eigenstate of $a$ with eigenvalue $\alpha$:

$$a|\alpha\rangle = e^{-\frac{1}{2}\overline{\alpha}\alpha}\sum_{n=0}^{\infty}\frac{\alpha^n}{\sqrt{n!}}a|n\rangle = \alpha e^{-\frac{1}{2}\overline{\alpha}\alpha}\sum_{n=1}^{\infty}\frac{\alpha^{n-1}}{\sqrt{(n-1)!}}|n-1\rangle = \alpha|\alpha\rangle$$

  It is not an eigenstate of $a^\dagger$: $a^\dagger|\alpha\rangle = e^{-\frac{1}{2}\overline{\alpha}\alpha}\sum_{n=0}^{\infty}\frac{\sqrt{n+1}\alpha^n}{\sqrt{n!}}|n+1\rangle = \frac{e^{-\frac{1}{2}\overline{\alpha}\alpha}}{\alpha}\sum_{n=1}^{\infty}\frac{n\alpha^n}{\sqrt{n!}}|n\rangle$

- Although normalized, they are not orthogonal:

$$\langle\beta|\alpha\rangle = e^{-\frac{1}{2}\overline{\beta}\beta-\frac{1}{2}\overline{\alpha}\alpha}\sum_{n=0}^{\infty}\sum_{m=0}^{\infty}\frac{\overline{\beta}^n}{\sqrt{n!}}\frac{\alpha^m}{\sqrt{m!}}\langle n|m\rangle = e^{-\frac{1}{2}\overline{\beta}\beta-\frac{1}{2}\overline{\alpha}\alpha}\sum_{n=0}^{\infty}\frac{(\overline{\beta}\alpha)^n}{n!} = e^{-\frac{1}{2}\overline{\beta}\beta-\frac{1}{2}\overline{\alpha}\alpha+\overline{\beta}\alpha}$$

- Time Evolution: $|\alpha(t)\rangle = e^{-\frac{1}{2}\overline{\alpha}\alpha}\sum_{n=0}^{\infty}\frac{\alpha^n}{\sqrt{n!}}|n(t)\rangle$ The evolving eigenstate is

$$|n(t)\rangle = e^{-i\frac{E_n t}{\hbar}}|n(0)\rangle = e^{-i\frac{1}{2}\omega t}e^{-in\omega t}\frac{(a^\dagger)^n}{\sqrt{n!}}|0\rangle$$

  If we denote $a^\dagger(t) = a^\dagger(0)e^{-i\omega t}$, then we have a similar form $|n(t)\rangle = e^{-i\frac{1}{2}\omega t}\frac{(a^\dagger(t))^n}{\sqrt{n!}}|0\rangle$, where the initial $e^{-i\frac{1}{2}\omega t}$ is a global phase term and does not change the physical meaning (matrix elements) of the state.

- Matrix element of coordinate: $\langle\alpha|x|\alpha\rangle$, using

$$x = \sqrt{\frac{\hbar}{2m\omega}}(a+a^\dagger), \qquad \langle\alpha|a^\dagger = (a|\alpha\rangle)^\dagger = \langle\alpha|\overline{\alpha}$$

  If $a, a^\dagger$ are changed to be time-dependent, then $a|\alpha\rangle = \alpha e^{i\omega t}|\alpha\rangle$, and the matrix element is:

$$\langle\alpha(t)|x|\alpha(t)\rangle = \sqrt{\frac{\hbar}{2m\omega}}(\alpha e^{i\omega t} + \overline{\alpha}e^{-i\omega t}) \tag{15}$$

  This is a periodically oscillating real number, describing the classical harmonic oscillator equation of motion. $\alpha$ corresponds to the amplitude of this oscillator.

- Wavefunction broadening: Consider $\langle\alpha(t)|\, x^2\, |\alpha(t)\rangle = \dfrac{\hbar}{2m\omega}\langle\alpha(t)|\,(a+a^\dagger)^2\,|\alpha(t)\rangle$ where

$$\langle\alpha|\, a^2\,|\alpha\rangle = (\alpha e^{i\omega t})^2, \langle\alpha|\,(a^\dagger)^2\,|\alpha\rangle = (\overline{\alpha}e^{-i\omega t})^2, \langle\alpha|\, a^\dagger a\,|\alpha\rangle = (\overline{\alpha}e^{-i\omega t})(\alpha e^{i\omega t}) = \overline{\alpha}\alpha$$

$$\langle\alpha|\, aa^\dagger\,|\alpha\rangle = \left(\frac{e^{-\frac{1}{2}\overline{\alpha}\alpha}}{\overline{\alpha}}\sum_{n=1}^{\infty}\frac{n\overline{\alpha}^n}{\sqrt{n!}}\langle n|\, e^{i\omega t}\right)\left(\frac{e^{-\frac{1}{2}\overline{\alpha}\alpha}}{\alpha}\sum_{n=1}^{\infty}\frac{n\alpha^n}{\sqrt{n!}}|n\rangle\, e^{-i\omega t}\right) = \frac{e^{-|\alpha|^2}}{\alpha^2}\sum_{n=1}^{\infty}\frac{n^2(\overline{\alpha}\alpha)^n}{n!}$$

$$= e^{-\frac{1}{2}|\alpha|^2}\sum_{n=0}^{\infty}\frac{(n+1)(\overline{\alpha}\alpha)^n}{n!} = e^{-|\alpha|^2}\left(\sum_{n=0}^{\infty}\frac{(\overline{\alpha}\alpha)^n}{n!}+\sum_{n=1}^{\infty}\frac{(\overline{\alpha}\alpha)^n}{(n-1)!}\right)$$

$$= e^{-|\alpha|^2}(e^{\overline{\alpha}\alpha}+\overline{\alpha}\alpha e^{\overline{\alpha}\alpha}) = 1+\overline{\alpha}\alpha$$

  Substituting in gives: $\langle\alpha(t)|\, x^2\,|\alpha(t)\rangle = \dfrac{\hbar}{2m\omega}\left(1+2\overline{\alpha}\alpha+\alpha^2e^{i2\omega t}+\overline{\alpha}^2e^{-2i\omega t}\right)$, so the variance of the coordinate is:

$$\mathbb{D}(x^2) = \langle\alpha(t)|\, x^2\,|\alpha(t)\rangle - (\langle\alpha(t)|\, x\,|\alpha(t)\rangle)^2$$

$$= \frac{\hbar}{2m\omega}\left(1+2\overline{\alpha}\alpha+\alpha^2e^{i2\omega t}+\overline{\alpha}^2e^{-2i\omega t}\right) - \frac{\hbar}{2m\omega}(\alpha e^{i\omega t}+\overline{\alpha}e^{-i\omega t})^2$$

$$= \frac{\hbar}{2m\omega}$$

  This shows that the coherent state wavefunction does not broaden over time.

### 5.2.2 Exponential Commutation Relations

In mathematics, the Baker–Campbell–Hausdorff formula describes the exponential operation of non-commuting operators (although not covered in class, it is necessary to introduce it for the proof above):

$$e^Xe^Y = e^Z, Z = X+Y+\frac{1}{2}[X,Y]+\frac{1}{3!}(\frac{1}{2}[X,[X,Y]]+\frac{1}{2}[[X,Y],Y])+...$$

If the commutator result $[X,Y]$ is a constant, then the formula can be simplified to the following form (Note: using the property that $[X,Y]$ commutes with both $X$ and $Y$):

$$e^{X+Y} = e^{-\frac{1}{2}[X,Y]}e^Xe^Y$$

Using the above result, Eq. 14 can be proven: Let $X = \alpha a^\dagger, Y = -\overline{\alpha}a$, $[X,Y] = \overline{\alpha}\alpha[a^\dagger,a] = -\overline{\alpha}\alpha$, then

$$e^{\alpha a^\dagger-\overline{\alpha}a}\,|0\rangle = e^{-\frac{1}{2}\overline{\alpha}\alpha}e^{\alpha a^\dagger}e^{-\overline{\alpha}a}\,|0\rangle$$

Since $a\,|0\rangle = 0$, $e^{-\overline{\alpha}a}\,|0\rangle = \sum_{n=0}^{\infty}\dfrac{\overline{\alpha}^n}{n!}a^n\,|0\rangle$, only the $n=0$ term is non-zero, so $e^{-\overline{\alpha}a}\,|0\rangle = |0\rangle$. Substituting this gives the expression to be proven:

$$|\alpha\rangle = e^{-\frac{1}{2}\overline{\alpha}\alpha}e^{\alpha a^\dagger}\,|0\rangle = e^{\alpha a^\dagger-\overline{\alpha}a}\,|0\rangle$$

### 5.3 Tensor Product

When learning field theory in the electrodynamics course, the concept of tensor product was introduced: Assuming $R^{\alpha_1 \ldots \alpha_n}$ and $S^{\beta_1 \ldots \beta_m}$ are tensors of rank n and m respectively, their tensor product is called

$$T^{\alpha_1 \ldots \alpha_n \beta_1 \ldots \beta_m} = R^{\alpha_1 \ldots \alpha_n} S^{\beta_1 \ldots \beta_m}$$

which is a tensor of rank $n + m$.

In this report, the tensor $s \otimes t$ is mentioned. Let $s$ be represented by subscript $n$ ($s_n = |n\rangle_s$), and $t$ by subscript $i$ ($t_i = |i\rangle_{e0}$), then $(s \otimes t)_{ni} = |n\rangle_s |i\rangle_{e0}$. Similarly, the tensor product in the Hamiltonian (Eq. 2) can also be embodied by matrix elements:

$$\langle j|_{e0} \langle m|_s H |n\rangle_s |i\rangle_{e0} = \langle m|_s H_s |n\rangle_s \times 1 + \langle m|_s q_s |n\rangle_s \times \langle j|_{e0} H_e^I |i\rangle_{e0} + 1 \times \langle j|_{e0} H_e |i\rangle_{e0} \quad (16)$$

## References


[1] Andreas Albrecht. "Equilibration and "Thermalization" in the Adapted Caldeira–Leggett Model". In: *Entropy* 24.3 (2022). ISSN: 1099-4300. DOI: 10.3390/e24030316. URL: https://www.mdpi.com/1099-4300/24/3/316.

[2] Andreas Albrecht, Rose Baunach, and Andrew Arrasmith. "Adapted Caldeira-Leggett model". In: *Phys. Rev. Res.* 5 (2 2023), p. 023187. DOI: 10.1103/PhysRevResearch.5.023187. URL: https://link.aps.org/doi/10.1103/PhysRevResearch.5.023187.

[3] Andreas Albrecht, Rose Baunach, and Andrew Arrasmith. "Einselection, equilibrium, and cosmology". In: *Physical Review D* 106 (Dec. 2022). DOI: 10.1103/PhysRevD.106.123507.

[4] Andreas Albrecht and Alberto Iglesias. "Clock ambiguity and the emergence of physical laws". In: *Phys. Rev. D* 77 (6 Mar. 2008), p. 063506. DOI: 10.1103/PhysRevD.77.063506. URL: https://link.aps.org/doi/10.1103/PhysRevD.77.063506.

[5] Andreas Albrecht and Alberto Iglesias. "Lorentz symmetric dispersion relation from a random Hamiltonian". In: *Phys. Rev. D* 91 (4 Feb. 2015), p. 043529. DOI: 10.1103/PhysRevD.91.043529. URL: https://link.aps.org/doi/10.1103/PhysRevD.91.043529.

[6] A.O Caldeira and A.J Leggett. "Quantum tunnelling in a dissipative system". In: *Annals of Physics* 149.2 (1983), pp. 374–456. ISSN: 0003-4916. DOI: https://doi.org/10.1016/0003-4916(83)90202-6. URL: https://www.sciencedirect.com/science/article/pii/0003491683902026.

[7] A.O. Caldeira and A.J. Leggett. "Path integral approach to quantum Brownian motion". In: *Physica A: Statistical Mechanics and its Applications* 121.3 (1983), pp. 587–616. ISSN: 0378-4371. DOI: https://doi.org/10.1016/0378-4371(83)90013-4. URL: https://www.sciencedirect.com/science/article/pii/0378437183900134.

[8] *Eigenstate thermalization hypothesis - Wikipedia*. URL: https://en.wikipedia.org/wiki/Eigenstate_thermalization_hypothesis.

[9] Rahul Nandkishore and David A. Huse. "Many-Body Localization and Thermalization in Quantum Statistical Mechanics". In: *Annual Review of Condensed Matter Physics* 6.Volume 6, 2015 (2015), pp. 15–38. ISSN: 1947-5462. DOI: https://doi.org/10.1146/annurev-conmatphys-031214-014726. URL: https://www.annualreviews.org/content/journals/10.1146/annurev-conmatphys-031214-014726.

[10] Juan Pablo Paz and Wojciech Hubert Zurek. "Quantum Limit of Decoherence: Environment Induced Superselection of Energy Eigenstates". In: *Phys. Rev. Lett.* 82 (26 June 1999), pp. 5181–5185. DOI: 10.1103/PhysRevLett.82.5181. URL: https://link.aps.org/doi/10.1103/PhysRevLett.82.5181.

[11] Sandu Popescu, Anthony J. Short, and Andreas Winter. “Entanglement and the foundations of statistical mechanics”. In: *Nature Physics* 2 (11 2006), pp. 754–758. ISSN: 1745-2481. DOI: 10.1038/nphys444. URL: https://doi.org/10.1038/nphys444.

[12] Mark Srednicki. “Chaos and quantum thermalization”. In: *Phys. Rev. E* 50 (2 Aug. 1994), pp. 888–901. DOI: 10.1103/PhysRevE.50.888. URL: https://link.aps.org/doi/10.1103/PhysRevE.50.888.

[13] Wojciech H. Zurek, Salman Habib, and Juan Pablo Paz. “Coherent states via decoherence”. In: *Phys. Rev. Lett.* 70 (9 Mar. 1993), pp. 1187–1190. DOI: 10.1103/PhysRevLett.70.1187. URL: https://link.aps.org/doi/10.1103/PhysRevLett.70.1187.

[14] Robert Zwanzig. “Nonlinear generalized Langevin equations”. In: *Journal of Statistical Physics* 9 (3 1973), pp. 215–220. ISSN: 1572-9613. DOI: 10.1007/BF01008729. URL: https://doi.org/10.1007/BF01008729.